

A Comprehensive Survey of Action Quality Assessment: Method and Benchmark

Kanglei Zhou¹, Ruizhi Cai¹, Liyuan Wang¹, Hubert P. H. Shum², *Senior Member, IEEE*, Xiaohui Liang¹

Abstract— Action Quality Assessment (AQA) quantitatively evaluates the quality of human actions, providing automated assessments that reduce biases in human judgment. Its applications span domains such as sports analysis, skill assessment, and medical care. Recent advances in AQA have introduced innovative methodologies, but similar methods often intertwine across different domains, highlighting the fragmented nature that hinders systematic reviews. In addition, the lack of a unified benchmark and limited computational comparisons hinder consistent evaluation and fair assessment of AQA approaches. In this work, we address these gaps by systematically analyzing over 150 AQA-related papers to develop a hierarchical taxonomy, construct a unified benchmark, and provide an in-depth analysis of current trends, challenges, and future directions. Our hierarchical taxonomy categorizes AQA methods based on input modalities (video, skeleton, multi-modal) and their specific characteristics, highlighting the evolution and interrelations across various approaches. To promote standardization, we present a unified benchmark, integrating diverse datasets to evaluate the assessment precision and computational efficiency. Finally, we review emerging task-specific applications and identify under-explored challenges in AQA, providing actionable insights into future research directions. This survey aims to deepen understanding of AQA progress, facilitate method comparison, and guide future innovations. The project web page can be found at <https://ZhouKanglei.github.io/AQA-Survey>.

Index Terms—Action Quality Assessment, Sports Scoring, Skill Assessment, Physical Exercise Assessment

arXiv:2412.11149v1 [cs.CV] 15 Dec 2024

1 INTRODUCTION

ACTION Quality Assessment (AQA) [1], [2], [3], [4], [5] evaluates the quality of performed actions, offering an objective alternative to subjective human assessments. Since its introduction by Gordon et al. [6], AQA has become indispensable for addressing challenges in human judgment, reducing biases, and minimizing the costs associated with expert evaluations. Its adoption spans diverse domains such as sports analysis [7], [8], [9], [10], medical care [11], [12], [13], and skill evaluation [14], [15]. Unlike action recognition [16], [17], [18], [19] that identifies *what* action is performed, AQA emphasizes *how well* it is executed. This requires domain-specific criteria, interpretable outputs, and sensitivity to subtle performance differences, which traditional computer vision methods do not address.

Recent advancements in deep learning [23] have driven significant progress in AQA (see Fig. 1(a)). These developments have introduced innovative methodologies and expanded applications (see Fig. 1(b)). However, the diversity of domains and intertwined approaches in AQA com-

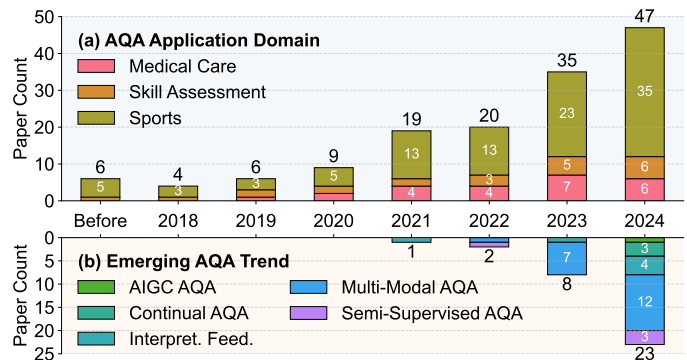


Fig. 1: Annual statistics of AQA papers in CV and ML conferences or journals, categorized by (a) AQA application domains and (b) emerging research directions in AQA that have often been overlooked in previous surveys. The notable rise in publications and the evolving trends in recent years highlight the need for a comprehensive survey.

plicates systematic reviews. Although prior surveys [20], [21], [22] have attempted to summarize advancements in AQA, they lack comprehensive coverage across multiple dimensions, as highlighted in Tab. 1. First, these surveys often focus narrowly on specific domains, offering incomplete perspectives that overlook interrelations across diverse AQA applications. In addition, their taxonomies in [20], [21] categorize AQA approaches by application domains, failing to capture the progression of diverse methodologies. For instance, sports analysis and skill assessment often share video-based inputs, yet treating their methods separately overlooks shared techniques, resulting in fragmented reviews. Second, existing AQA methods [24], [25] lack a unified and standardized benchmark in evaluation protocols, datasets, and metrics, leading to inconsistent comparisons and fragmented progress. Furthermore, computational per-

- K. Zhou and R. Cai are with the State Key Laboratory of Virtual Reality Technology and Systems, Beihang University, Beijing, China. E-mail: zhoukanglei@buaa.edu.cn, craaaaazy@buaa.edu.cn
- L. Wang is with the Department of Computer Science and Technology, Institute for AI, BNRist Center, THBI Lab, Tsinghua-Bosch Joint Center for ML, Tsinghua University, Beijing 100190, China. E-mail: wly19@tsinghua.org.cn
- H. Shum is with the Department of Computer Science, Durham University, Durham DH1 3LE, United Kingdom. E-mail: hubert.shum@durham.ac.uk
- X. Liang is with the State Key Laboratory of Virtual Reality Technology and Systems, Beihang University, Beijing, China, and also with Zhong-guancun Laboratory, Beijing, China. E-mail: liang_xiaohui@buaa.edu.cn

(Corresponding author: Xiaohui Liang.)

TABLE 1

Comparison of existing AQA surveys across multiple dimensions. 🏊, 🏥, and 🧑‍🎓 indicate sports, medical care, and skill assessment icons. † and ‡ denote two-level taxonomy standards. 📺, 🦴, 📄, 🎧, 👁, and 📊 represent video, skeleton, text, audio, gaze, and flow icons. The fewer the ★ ratings, the less unified the benchmark becomes for fair evaluation and comparison. 📁 and 📏 denote the dataset and metric icons.

Survey	Year	Domains	Taxonomy	Modality	Benchmark	Core Contributions
Lei et al. [20]	2019	🏊 🏥 🧑‍🎓	† Feature type, ‡ Domain	📺 🦴	★★★☆☆: 3 📁 with 2 📏	Comprehensive overview of motion detection and data preprocessing in AQA.
Wang et al. [21]	2021	🏊 🏥	† Domain, ‡ Feature type	📺	★☆☆☆☆: No evaluations	Emphasized categorization by publishing institutions and fields of application.
Liu et al. [22]	2024	🏊 🏥 🧑‍🎓	† Input mode	📺 🦴 📄 🎧	★★★☆☆: 3 📁 with 1 📏	A detailed review of 96 papers, including their applications, methods, etc.
Ours	2024	🏊 🏥 🧑‍🎓	† Input mode, ‡ Mode specialty	📺 🦴 📄 🎧 👁 📊 ...	★★★★★: 6 📁 with 7 📏 Unified setting	A well-designed taxonomy of over 150 papers, a unified benchmark, specific AQA tasks, challenges, and prospects.

formance is frequently overlooked in method evaluations, creating gaps in assessing the practicality of different approaches. Third, even the most recent survey [22] neglect recent advancements in multi-modal AQA [26], [27], [28], [29], as well as significant progress in leveraging semi-supervised learning techniques [30], [31], adapting to non-stationary variations [32], [33], [34], and generating interpretable feedback [24], [27], [35] rather than solo quality scores. These gaps necessitate a comprehensive survey that integrates recent advancements and establishes a unified benchmark for consistent evaluation and comparison.

To address the pressing need, this survey comprehensively reviews advancements in AQA by analyzing over 150 AQA-related papers to develop a hierarchical taxonomy, construct a unified benchmark, and provide an in-depth analysis of current trends, challenges, and future directions. First, we argue that the type of input data, rather than the application domain, is the primary determinant of AQA model design. Based on this premise, we propose a hierarchical taxonomy. Specifically, we categorize approaches into video-based, skeleton-based, and multi-modal methods, further distinguishing them by modality-specific attributes. Second, we establish a unified AQA benchmark, the largest to our knowledge, integrating six widely used datasets and seven evaluation metrics. By standardizing experimental settings, we facilitate consistent comparisons across diverse methods, evaluating both accuracy and the often-overlooked computation overhead. Finally, we review emerging task-specific AQA applications and identify under-explored challenges. By incorporating cross-directional knowledge, we offer actionable insights to guide future advancements. Our contributions are:

- We conduct an in-depth analysis of the development of AQA by using a novel hierarchical taxonomy that categorizes methods based on input modalities and their distinct characteristics. This enables a clearer understanding of the progression and interconnections within AQA approaches.
- We establish the largest, open-sourced, unified framework for benchmarking AQA methods by systematically analyzing widely used datasets and experimental protocols. This framework facilitates consistent evaluation and comparison across approaches by assessing accuracy and computational efficiency.
- We highlight three task-specific applications of AQA that address critical real-world challenges, extending

beyond traditional AQA settings. Additionally, we identify under-explored challenges, offering actionable insights into potential research directions to advance the field in practical scenarios.

The remainder of this paper is structured in Fig. 2. Sec. 2 introduces the foundational setup. Sec. 3 provides an in-depth analysis of typical AQA methods, while Sec. 4 reviews available datasets and presents the unified benchmark framework. Sec. 5 highlights key task-specific applications. Sec. 6 explores current trends and outlines future research directions. Finally, Sec. 7 summarizes the paper.

2 FUNDAMENTALS OF COMMON AQA SETUP

In this section, we first formulate a common AQA framework designed to accommodate multi-modal inputs. Then we introduce typical scenarios and their evaluation metrics.

2.1 Problem Formulation

Fig. 3 illustrates the unified framework for AQA, focusing on evaluating the quality of actions through diverse input modalities, including video, skeleton data, and sensor inputs. Let $\mathcal{X} = \{\mathbf{X}^{(1)}, \mathbf{X}^{(2)}, \dots, \mathbf{X}^{(M)}\}$ represent a set of $M \geq 1$ input modalities, where each $\mathbf{X}^{(m)} = [\mathbf{x}_1^{(m)}; \mathbf{x}_2^{(m)}; \dots; \mathbf{x}_T^{(m)}]$ corresponds to a sequence of observations for modality m over time $t \in \{0, 1, \dots, T\}$. The AQA process in a neural network architecture can be divided into three primary components: feature extraction (backbone), representation learning layer (neck), and score prediction (head). Each input modality $\mathbf{X}^{(m)}$ is processed through a feature extractor $f_m(\cdot)$, generating modality-specific features $\mathbf{F}^{(m)} = f_m(\mathbf{X}^{(m)})$. Then the extracted features are passed through the neck $g(\cdot)$, which fuses and transforms the features into an overall representation $\mathbf{Z} = g(\mathbf{F}^{(1)}, \mathbf{F}^{(2)}, \dots, \mathbf{F}^{(M)})$. Finally, the learned representation \mathbf{Z} is passed through a quality prediction head $h(\cdot)$ to estimate the predicted quality score $\hat{y} = h(\mathbf{Z})$. Finally, the overall function can be expressed as:

$$\hat{y} = h\left(g\left(f_1\left(\mathbf{X}^{(1)}\right), f_2\left(\mathbf{X}^{(2)}\right), \dots, f_M\left(\mathbf{X}^{(M)}\right)\right)\right). \quad (1)$$

Our formulation retains generality and can handle both uni-modal and multi-modal AQA methods. For uni-modal methods ($M = 1$), the focus is on a single input type, such as video (see Sec. 3.1) or skeletal data (see Sec. 3.2), which provide fully human-centric cues crucial for AQA and can

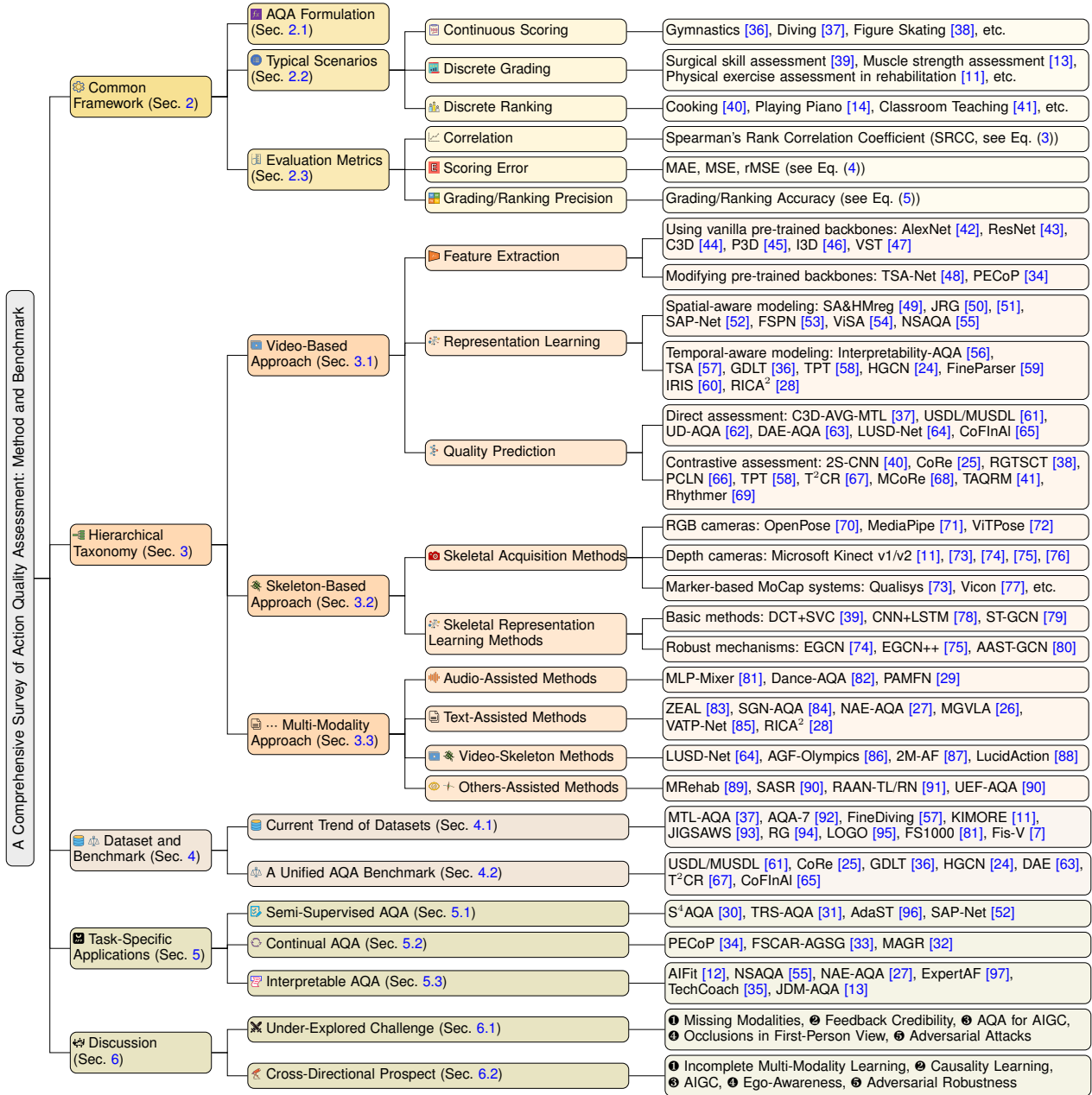


Fig. 2: The overall structure of our comprehensive survey. Our survey presents three core contributions: a **hierarchical taxonomy** systematically organizing intertwined papers with in-depth analysis, a **unified benchmark** to ensure consistent evaluation and fair comparison, and an exploration of **task-specific applications** in AQA beyond common setup, **under-explored challenges**, and **prospects**.

be used independently for assessment. For multi-modal methods ($M > 1$), auxiliary modalities, such as audio and text, assist them in comprehensive analysis (see Sec. 3.3).

2.2 Typical Scenarios

In AQA, the form of the output varies depending on the requirements of different applications. Broadly, AQA methods can produce two types of outputs: continuous scores and discrete categories (such as grades or ranks).




2.2.1 Continuous Score: Continuous scores are commonly used in scenarios that require precise and detailed evaluation, such as in Olympic sports performance assessments [7], [36], [37], [38], [98]. The score \hat{y} in Eq. (1) typically ranges within a specific interval, $[a, b]$ (e.g., $[0, 100]$), reflecting the exact quality of the action. The primary objective is to

predict a continuous numerical value that accurately quantifies action quality, providing precise feedback essential for competitive evaluation and improvement.

2.2.2 Discrete Grade or Rank: Discrete outputs simplify the assessment by grouping performances into predefined levels or relative rankings, making evaluation more interpretable for scenarios where exact performance scores are not available or essential. **Grading** assigns the action performance to a discrete level $\hat{y} \in \{1, 2, \dots\}$, such as “excellent”, “good”, “fair”, or “poor”. This approach is suitable for cases where a coarse but clear evaluation is needed, such as in skill assessment applications [39], [83], [99], [100]. Grading reduces the complexity of continuous scoring by grouping similar performances into broader categories. **Ranking**

TABLE 2

Comparison of AQA scenarios, outlining their output formats, the precision of feedback, the complexity of annotation, and the application suitability.

Scenarios	Outputs	Precision of Feedback	Complexity of Annotation	Application Suitability
Continuous Scoring	 $\hat{y} \in [a, b]$	★★★: Delivers highly exact feedback under certain criterion	★★★: Requires precise annotations often from domain experts	Sports (e.g., gymnastics [36], diving [37], figure skating [38])
Discrete Grading	 $\hat{y} \in \{1, 2, \dots\}$	★★☆: Offers output that is easier to interpret but less granular	★★☆: Demands annotations with moderate granularity	Skill assessment (e.g., surgery [39], physical exercise [11])
Discrete Ranking	 $\hat{y} \in \{-1, 0, 1\}$	★☆☆: Provides general feedback with limited detail	★☆☆: Requires minimal effort	Niche competitive tasks (e.g., cooking [40], playing piano [14])

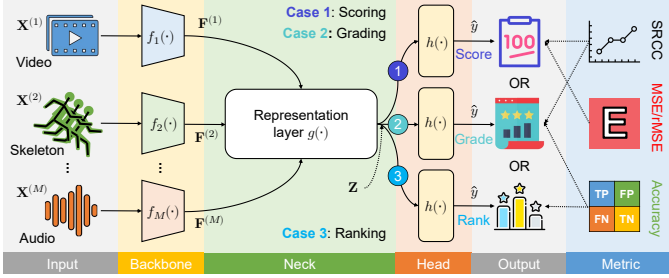


Fig. 3: Illustration of the common AQA framework, consisting of three core components: (1) the backbone for feature extraction, which processes diverse input data modalities such as video, skeleton, or sensor data; (2) the network neck for representation learning, responsible for deriving meaningful embeddings from the extracted features; and (3) the regression or classification head, which generates outputs as continuous scores (Case 1), discrete grades (Case 2), or ranks (Case 3).

establishes a relative order of performances by comparing them against each other. This method is useful in pairwise or group comparisons [40], [41], [69], where absolute scores are less important, and the goal is to determine who performed better. Note that Fig. 3 does not include the paired data for ranking to enhance clarity; a detailed process is provided in Fig. 6. Given paired data from sample i and j , the pairwise ranking model in Eq. (1) typically generates:

$$\hat{y}_{(i,j)} = \begin{cases} 1, & i \text{ shows higher skill than } j, \\ -1, & i \text{ shows lower skill than } j, \\ 0, & \text{no skill preference.} \end{cases} \quad (2)$$

This output encodes the relative skill comparison between the two samples. The ranking assesses performance without assigning specific numerical values, often preferred in competitive scenarios where only the relative position matters.

Typically, AQA tasks rely on fully labeled training samples with a single output, representing supervised AQA, as summarized in Tab. 2. Recent advancements have expanded AQA into semi-supervised [30], [31], [52], continual learning [32], [33], and interpretable [13], [55], [97] scenarios. These evolving settings are detailed in Sec. 5.

2.3 Evaluation Metrics

Evaluating model performance for AQA is essential for understanding its effectiveness across various applications. Generally, two primary categories of evaluation metrics are employed: correlation metrics and precision metrics.

2.3.1 Correlation Metrics: The primary correlation metric used in AQA is the Spearman Rank Correlation Coefficient (SRCC). This metric assesses the strength and direction of the relationship between the predicted scores

\hat{y}_i ($i \in \{1, 2, \dots, N\}$) and the true scores y_i based on their ranks \hat{r}_i and r_i . SRCC can be defined as:

$$\text{SRCC} = \frac{\sum_{i=1}^N (r_i - \bar{r})(\hat{r}_i - \bar{\hat{r}})}{\sqrt{\sum_{i=1}^N (r_i - \bar{r})^2} \sqrt{\sum_{i=1}^N (\hat{r}_i - \bar{\hat{r}})^2}}, \quad (3)$$

where \bar{r} and $\bar{\hat{r}}$ are the mean ranks of true and predicted scores, respectively. SRCC is particularly useful in scenarios where the precise numerical score is less important than the relative ranking of actions. This makes it a robust metric for evaluating ordinal data, as it emphasizes the consistency of rankings rather than absolute values.

2.3.2 Precision Metrics: Two common types of precision metrics assess the accuracy of predicted scores, tailored to either continuous or discrete outputs (see Sec. 2.2).

Score error quantifies the difference between the predicted and actual scores, allowing for an assessment of the model’s accuracy in predicting continuous quality scores. Common measures include Mean Absolute Error (MAE) and Mean Squared Error (MSE), which provide insights into the magnitude of prediction errors. Recently, relative Mean Squared Error (rMSE) [24], [25] has gained popularity as it avoids the impact of differing score scales across actions in different categories. rMSE can be represented as:

$$\text{rMSE} = \frac{1}{N} \sum_{i=1}^N \left(\frac{y_i - \hat{y}_i}{y_{\max} - y_{\min}} \right)^2 \times 100, \quad (4)$$

where y_{\max} and y_{\min} denote the maximum and minimum scores, respectively. Note that our definition differs slightly from the relative ℓ_2 in [25]. Normalization scales the score to a decimal, and squaring reduces it further. To address this, we multiply by 100 to re-scale it to a range of 0 to 1.

Accuracy measures the proportion of correctly predicted grades or ranked pairs relative to the total predictions made for applications where actions are categorized into discrete grades or ranks, which can be represented as:

$$\text{Accuracy} = \frac{\sum_{i=1}^N \mathbb{1}(\hat{y}_i = y_i)}{N} \times 100\%, \quad (5)$$

where $\mathbb{1}(\cdot)$ denotes the indicator function, which equals 1 if $\hat{y}_i = y_i$ and 0 otherwise. This metric is essential in scenarios where precise classification is crucial for evaluating performance levels, such as grades or ranks.

For general AQA, employing both correlation and precision metrics provides a comprehensive evaluation of a model’s performance. Indeed, beyond the commonly used metrics, custom metrics are sometimes employed for specialized tasks. For instance, certain AQA methods [57], [59], [108] that incorporate temporal segmentation use Intersection over Union (IoU) for evaluation.

TABLE 3
Backbones commonly used in video-based AQA approach and their key characteristics.

Backbone	Type	Typical Works	Pre-Trained Dataset	Spatial-Temporal Modeling	Efficiency	Generalization
AlexNet [42]	2D CNN	[40]	ImageNet [42]	★☆☆☆☆: Basic spatial with simple conv., no explicit temporal design	★★★★★: High due to simplicity	★★★☆☆: Limited in generalization
ResNet [43]	2D CNN	[101], [102]	ImageNet [42]	★★★★☆: Excels in spatial extraction, no explicit temporal design	★★★★☆: Balanced for deep layers	★★★★☆: Good for mitigating overfitting
C3D [44]	3D CNN	[92], [98]	Sports1M [44]	★★★★☆: Good with 3D conv.	★★☆☆☆: Heavy 3D	★★★☆☆: Moderate
P3D [45]	3D CNN	[103], [104], [105]	Kinetics-400 [46]	★★★★☆: Balanced for separate spatial and temporal conv. layers	★★★★☆: Higher than 3D CNNs	★★★☆☆: Less for its hybrid design
I3D [46]	3D CNN	[24], [50], [58], [59], [62], [106]	Kinetics-400 [46]	★★★★★: Strong by inflating 2D conv. into 3D conv.	★★★★☆: High resources for 3D conv.	★★★★☆: Good for various tasks
VST [47]	Transformer	[36], [56], [65], [84]	Kinetics-600 [107]	★★★★★: Good spatial, advanced long-range temporal dependencies	★★☆☆☆: High for self-attention	★★★★☆: Good for complex scenarios

3 METHODS WITH A HIERARCHICAL TAXONOMY

This section presents a taxonomy of representative AQA methods categorized by input modalities: video-based (see Sec. 3.1), skeleton-based (see Sec. 3.2), and multi-modality (see Sec. 3.3) methods. Input type significantly impacts model design, as each modality requires tailored architectures to effectively capture relevant features for accurate quality assessment. We further classify each approach based on its distinctive characteristics, exploring how different inputs are processed. The primary motivations, typical implementations, and empirical properties of these methods are analyzed, providing a comprehensive overview of the advantages and trade-offs in performance and application.

3.1 Video-Based Approach

When $M = 1$ and $\mathbf{X}^{(1)} \in \mathbb{R}^{T \times H \times W \times 3}$ represents the video input, where T, W, H and 3 denote the number of frames, width, height, and color channels, respectively, Eq. (1) corresponds to video-based approaches [109], [110]. These methods leverage detailed visual data to capture fine-grained motion dynamics and contextual cues, such as surroundings and object interactions, making them particularly effective for evaluating complex, visually dependent tasks, such as gymnastics and diving. Different approaches focus on distinct aspects: some emphasize feature extraction to capture critical patterns, others prioritize video-level representation learning to improve spatial-temporal modeling, and various approaches refine quality prediction techniques to handle the subtle details of action execution. Organizing the review around feature extraction, video-level representation learning, and quality prediction helps highlight how each approach addresses the unique challenges.

3.1.1 Feature Extraction: In the realm of AQA, effective feature extraction is vital for accurate action assessment. Early methods [18], [111], [112], [113], [114], [115], [116], [117], [118] primarily relied on handcrafted features such as spatial-temporal interest points (STIP) [119] used in [116], histogram of gradients (HOG) [120] employed in [115], [116], histogram of optical flow (HOF) [121] applied in [115], [116], and scale-invariant feature transform (SIFT) [17] used in [112]. However, these methods often struggled to fully capture the rich visual and temporal cues essential for AQA and tended to generalize poorly across different domains.

Utilizing Vanilla Pre-Trained Backbones. With the advent of deep learning, feature extraction backbones for AQA have evolved significantly (see Tab. 3). One of the key challenges is balancing computation efficiency with the

need to process high-redundancy video data, particularly in small-scale datasets where labeled samples are scarce due to the high annotation cost in AQA tasks. To mitigate these challenges, transfer learning is frequently employed, leveraging pre-trained backbones from large-scale image or action recognition datasets [42], [44], [107], [122] to extract robust features. Compared to 2D backbones like AlexNet [42] used in [40] and ResNet [43] applied in [101], [102], 3D CNNs are more effective at capturing spatial-temporal features. Models such as C3D [44] employed in [1], [92], [98], P3D [45] applied in [103], and I3D [46] used in recent studies [24], [50], [58], [59], [62], [106], process both spatial and temporal information simultaneously, offering a comprehensive understanding of action dynamics in videos. Among these, I3D stands out for its unique ability to inflate 2D convolutional filters into 3D, allowing it to capture motion dynamics and temporal dependencies more effectively. Its pre-training on large-scale action recognition datasets [107], [122] enhances its transferability to small-scale AQA tasks. Recently, the introduction of transformer-based models [36], [56], [65], [84], such as VST [47], has further improved feature extraction. Although these models provide more powerful representations than CNNs, they come with significantly higher computation costs.

Despite the success, both 3D and transformer-based backbones present challenges. 3D CNNs bring higher computation overhead compared to 2D networks, and transformer-based models increase this further. Moreover, temporal down-sampling methods, such as selecting key fragments [100], are often employed to reduce computation load, but these approaches can lead to the loss of critical cues necessary for AQA due to the omission of important temporal information. The common practice of dividing videos into equal-length clips for separate processing poses difficulties in accurately evaluating longer action sequences, where essential contextual and temporal information might be lost. This compromise remains a significant challenge in AQA research (see Sec. 3.1.2 for a detailed literature review and discussion on solutions addressing this issue).

In addition, transferability is often challenged by domain shifts that arise when transitioning from broader pre-trained tasks, such as action recognition, to the more fine-grained requirements of AQA. Features extracted from broader tasks are often coarse and may not capture the intricate details required for accurate AQA [34], [65], limiting a model's performance without further adaptation. To address this, pre-trained backbones are typically fine-tuned on specific AQA datasets. Instead of pure fine-tuning, Roditakis et

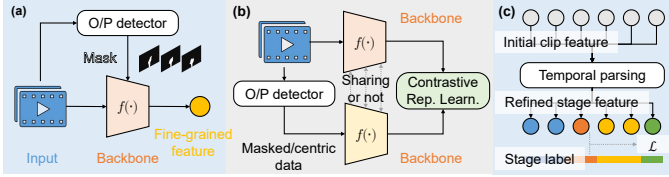


Fig. 4: Three typical fine-grained reasoning approaches in AQA. (a) This spatial reasoning method employs an off-the-shelf pose or object detector to generate object-centric masks, which are integrated into the intermediate layers of backbone networks, as seen in [48]. (b) This approach leverages a Siamese backbone that processes raw video alongside object- or pose-masked/centric data, using a contrastive learning module to direct attention toward object-centric regions [49], [52], [53]. Notably, certain methods [94], [126] opt for unshared parameters between the branches to facilitate the extraction of rich and hybrid features. (c) This fine-grained temporal-aware method typically incorporates a temporal parsing module to derive subactions, either implicitly or explicitly [24], [57], [59], [68].

al. [123] incorporated self-supervised TCC embeddings to align video sequences and complement appearance features during fine-tuning. Zhang et al. [96] introduced a method to transfer assessment skills from related source actions to a target action, allowing the model to adapt its features to the specific details of AQA tasks and improving its ability to capture task-specific patterns. However, these fine-tuning manners require considerable computation resources and a substantial amount of labeled samples to avoid overfitting. As a result, fine-tuned backbone methods are typically more suited to short-term AQA scenarios [25], [32], [37], [59], [124], especially when using 3D backbones, where the video length and computation complexity are manageable. In contrast, for minute-long videos [36], [56], [65], [84], where computation load becomes prohibitive, more powerful feature extractors such as VST [47] are usually preferred for their ability to handle longer sequences efficiently.

Modifying Pre-Trained Backbones. Two notable approaches [34], [48] address the domain shift challenge in AQA through backbone modifications, while other studies [65] focus on refining features via specialized representation layers to better capture task-specific details. TSA-Net [48] enhances spatial-temporal feature representation by inserting visual object tracker-generated masks [125] into the intermediate layers of I3D. This allows efficient human-centric information capture with sparse feature interactions, ensuring computation efficiency and flexibility. In contrast, PECoP [34] injects 3D into the inception modules of I3D and leverages self-supervised learning to learn in-domain spatiotemporal features, reducing domain shift while limiting parameter updates. Both approaches improve the adaptability of pre-trained models for fine-grained AQA tasks, which rely on capturing domain-specific details.

3.1.2 Video-Level Representation Learning: Video-level representation learning serves two main functions: refining extracted features to capture motion details more effectively and aggregating individual clip features into a cohesive video-level representation. This stage addresses key challenges from feature extraction, such as coarse features inherited from broader tasks and the loss of temporal context. By disentangling the spatial-temporal patterns of actions into finer spatial and temporal details and ensuring effective integration of clip-level information (see Fig. 4),

video-level representation learning helps mitigate these limitations, ultimately enhancing performance in AQA. In practice, each method contributes to both spatial and temporal modeling for AQA, though their primary focus may vary. In the following sections, we review papers centered on spatial-aware [49], [52], [53], [54] and temporal-aware [58], [92], [127], [128], [129], [130] approaches, respectively.

Spatial-Aware Modeling. The aim of *spatial-aware* action modeling is to prioritize object-centric features and critical contextual cues while minimizing the influence of irrelevant information such as backgrounds. Unlike TSA-Net [48], which modifies the feature extractor to enhance key feature focus (see Fig. 4(a)), two kinds of strategies [49], [50], [51], [52], [53], [54], [55] have emerged to enhance human-centric features for accurate AQA (see Fig. 4(b)).

The first strategy [49], [52] refines existing feature extractors by leveraging knowledge distillation to enhance attention to fine-grained cues, improving the model’s ability to capture subtle details in actions. For instance, Nagai et al. [49] developed a contrastive framework that incorporates a scene adversarial loss and a human-masked regression loss to guide the model’s attention toward human actions while suppressing background information. Similarly, SAP-Net [52] introduced a teacher-student network where the teacher branch focuses on the actor-centric region, generating high-quality pseudo-labels. These labels then assist the student branch in learning and inferring motion-oriented action features through consistency regularization, further enhancing the model’s ability to capture key action details.

The second strategy [50], [51], [54], [55], [95], [101], [109], [110] emphasizes refining broader feature representations by integrating additional cues for more accurate action evaluation. Li et al. [101] proposed an RNN-based spatial attention model that accumulates attention over frames and incorporates task progression to target critical regions in the video. Additionally, ViSA [54] classified video components into semantic categories such as tools, tissue, and background, enabling task-specific supervision for surgical skill assessment and enhancing evaluation in specialized domains. Instead of focusing on object-level features like [48], [52], Pan et al. [50], [51] utilized body part-level features obtained via pose estimation [131], constructing a spatial graph reasoning model on these parts for more fine-grained and precise action assessment. However, this method’s effectiveness is limited by the accuracy of the pose estimation process, particularly in the context of low-resolution and high-occlusion scenarios commonly found in Olympic videos. For multi-agent actions, Gao et al. [109], [110] utilized kinematic information to model asymmetric relationships between objects in surgical scenarios and athletes in synchronized diving. Similarly, GOAT [95] incorporated group formation features, enhancing synchronized swimming assessments by leveraging group-aware refinements.

Both strategies play a crucial role in refining fine-grained spatial feature representation, ultimately contributing to a more effective unified spatial-temporal model. Each presents unique advantages and disadvantages. Knowledge distillation [49], [52] effectively enhances targeted features relevant to human actions and improves generalization through a teacher-student framework, but it relies heavily on the quality of the teacher model and can introduce

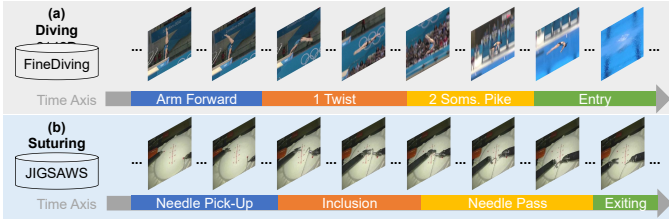


Fig. 5: The procedural nature of actions in fine temporal modeling for AQA. (a) illustrates a diving example from the FineDiving dataset [57], while (b) depicts a suturing example from the JIGSAWS dataset [93].

implementation complexity. In contrast, broad feature representation refinement [50], [51], [54], [101] promotes semantic awareness by accumulating attention over frames and grouping video components, allowing for a detailed analysis of complex actions. Ultimately, a hybrid approach that combines strengths from both strategies could lead to more robust and effective AQA models.

Temporal-Aware Modeling. The core of *temporal-aware* action modeling is often to leverage the procedural structure of actions (see Fig. 5) to tackle the challenge posed by disjoint clip features. An action typically consists of several subactions or procedures that unfold in a specific sequence [24], [57], [59], [105]. For example, in a diving action (see Fig. 5(a)), the sequence begins with the approach, followed by the takeoff, flight, and entry into the water. Each of these subactions is critical for evaluating the overall quality of the dive; misjudging any phase can lead to a lower score. However, inputs to the network that consist of equally sized clips often lack meaningful context. While straightforward methods, such as averaging clip-level features [98], are computationally simple, they frequently result in suboptimal performance due to vague temporal modeling and the loss of critical temporal dependencies. To address these limitations, both implicit techniques, which rely on networks to automatically learn sequential relationships from data, and explicit methods, designed to incorporate human knowledge through temporal annotations, have been developed to model the sequential dependencies between clips.

Implicit temporal modeling approaches [2], [24], [36], [58], [92], [96], [104], [127], [128], [129], [130], [132] rely on neural networks, such as LSTMs, which have been applied in early studies [92] to capture temporal dependencies between clips and enhance video-level representations (see Fig. 4(c) w/o stage labels). Building on previous approaches, more recent methods [36], [58], [127] have incorporated Transformers [133], which are particularly effective at modeling long-term dependencies, thereby improving the model’s ability to capture detailed aspects of action sequences. For example, Xu et al. [36] proposed GDLT by introducing grade decoupling using a Transformer decoder, which disentangles video features into grade-aware components via cross-attention between video features and learnable grade prototypes. Bai et al. [58] proposed a temporal parsing Transformer, using learnable queries tailored to specific actions, to extract fine-grained temporal representations with interpretable semantics. However, one challenge that arises with temporal sequences is the tendency of models to select shortcuts and skip decoder self-attention, leading to output degradation. This issue was addressed by Dong et al.

[56] by proposing an attention loss mechanism. Their solution facilitates mutual guidance between self-attention and cross-attention maps by minimizing the similarity between them using Kullback-Leibler (KL) divergence, thereby preventing performance degradation for accurate assessment.

Recently, the GCN-based HGNC [24] utilized structured video analysis knowledge to more effectively model both the temporal dynamics and relationships among clips. Additionally, some studies [68], [105], [134], [135], [136] have designed multi-stage temporal parsing networks to capture and analyze the sequential relationships between subactions more effectively, providing a deeper understanding of the temporal dynamics involved in complex actions. For instance, Liu et al. [129] and An et al. [68] proposed methods to evaluate sub-scores for each subaction, rather than aggregating all stages into a final score, enabling a more detailed assessment of action quality. In contrast to these methods, Gedamu et al. [53] introduced a Siamese network to encode both video and athlete-centric data extracted by an object detector [137]. Through contrastive learning between the two kinds of features, this approach mines subactions at a fine-grained level, facilitating the accurate parsing of subactions in an unsupervised manner.

On the other hand, *explicit* temporal modeling approaches, like TSA [57], [108] and FineParser [59], usually rely on manual annotations to guide the evaluation process, offering a more interpretable approach to temporal modeling in AQA (see Fig. 4(c) w/ stage labels). Xu et al. [57] initially developed a fine-grained FineDiving dataset structured by semantic and temporal levels. The coarse-grained annotations label action types, their temporal boundaries, and official scores, while the fine-grained level annotates each subaction step. They introduced a temporal segmentation attention module to enhance this structure. Later, they expanded the dataset with more data [108], further refining it through the addition of detailed human-centric foreground action masks in FineParser [59], improving assessment accuracy. In contrast, He et al. [138], [139] proposed a weakly supervised collaborative procedure alignment framework, leveraging instructional videos that share the same procedure. This approach exploits the inherent internal correlation between temporal steps of paired videos, reducing the need for exhaustive step-level annotations and improving AQA compared to TSA [57].

Both implicit and explicit methods present pros and cons. Implicit temporal modeling methods [24], [36], [58], [96], [127], [128], [129], [130], [132] excel in automatically capturing long-term dependencies and are highly flexible, capable of adapting to various AQA tasks without manual intervention. However, they often suffer from limited interpretability, higher computation demands, and a tendency to overfit, especially with small datasets. In contrast, explicit temporal modeling methods [57], [59], [108] provide more precise and interpretable assessments by relying on manually annotated subactions, enabling detailed analysis of specific action stages. Yet, they are labor-intensive, less scalable, and struggle to generalize across diverse datasets or unseen tasks. A hybrid approach combining them can harness both strengths, improving accuracy and interpretability.

3.1.3 Quality Prediction: The objective of quality prediction in AQA is to leverage fine-grained features to deliver

TABLE 4
Comparison of direct and contrastive assessment methods.

Assessment	Typical Works	Easy to Implement	Sensitivity to Variations	Required Data	Generalization	Computation
Direct	[55], [61], [62], [63], [92]	★★★★★: Simple	★★★☆☆: Limited ability to capture details	★★☆☆☆: Less for train	★★★★☆: Moderate	★★★★★: Efficient
Contrastive	[25], [40], [52], [57], [58], [140]	★★☆☆☆: Complex pairwise design	★★★★★: Robust for fine-grained assessments	★★★★★: More for pairs	★★★★☆: Better for relation focus	★★★☆☆: High for reference compute

comprehensive assessment feedback. This section reviews these methods: direct and contrastive assessments, distinguished by their respective strategies for evaluating action quality from video data. Direct and contrastive assessments offer distinct benefits and limitations (see Tab. 4). Direct assessments [24], [33], [37], [63], [65] directly map video features to a quality score, making them easy to implement. However, they often struggle to capture fine-grained performance differences, potentially overlooking subtle variations between high- and low-quality actions. Contrastive assessments [15], [40], [69], [140], [141], in contrast, excel at distinguishing these variations by comparing pairs of actions, improving sensitivity to subtle performance differences. Yet, they introduce complexity, requiring careful pair selection and additional computation resources. While direct assessments efficiently generate absolute scores, contrastive methods provide deeper insights but can complicate scoring and ranking processes.

Direct Assessment. Direct assessment methods [32], [37], [62], [63], [65], [142], [143] aim to predict an absolute quality score or grade for an action by minimizing the error between predicted and ground-truth values using regression or classification models. Some methods further refine the model’s sensitivity to quality differences, such as incorporating ranking loss [58], [100]. Although direct assessment is straightforward and often computationally efficient, it might struggle with generalization when action contexts vary or quality differences are subtle. To this end, researchers have proposed two key strategies: uncertainty modeling and subaction assessment.

The first strategy is *uncertainty modeling* of assessment [24], [28], [61], [62], [63], [64], [144]. Uncertainty modeling in AQA addresses the inherent ambiguity and variability in human judgment, acknowledging that even expert scores, while objective, can be influenced by subjective factors, leading to inconsistencies. This recognition has driven the development of models that predict multiple plausible scores instead of a single deterministic output, capturing a spectrum of potential assessment outcomes and enhancing the robustness of AQA by reflecting the natural variability in human assessment. The foundational work, USDL [61], introduces Gaussian distributions to soften single labels, enabling uncertainty modeling in regression. For multi-judge scenarios, MUSDL [61] extends USDL by employing a multi-path network to handle diverse evaluations. However, both methods rely on the known variance prior to label distribution, which may limit their applicability in scenarios without priors. Building on this, UD-AQA [62] focuses specifically on modeling the ambiguity inherent in expert evaluations of AQA tasks by employing CVAE [145] to generate multiple score predictions for each action. This approach not only produces a distribution of scores but also leverages uncertainty esti-

mates to re-weight the training loss and optimize the sample training order. Additionally, DAE [63] utilizes VAE-based techniques [146] to map video features into low-dimensional Gaussian distributions, directly outputting the final score through the re-parameterization trick, bypassing the need for neural network decoding. These methods collectively improve the robustness of AQA models by accounting for the uncertainty inherent in human assessments.

The second strategy is *subaction assessment* [28], [55], [60], [104], which enhances the generalization of AQA by decomposing complex actions into smaller, meaningful subactions, rather than relying solely on a video-level representation. A key challenge in this approach is the lack of subaction labels, which can make pseudo-labels [104] less convincing. To address this, Okamoto et al. [55] designed a model in which subaction outputs were validated by experts, ensuring high reliability. Specifically, Okamoto et al. quantify nine distinct aspects of a dive, assigning percentage scores where 100% denotes no error, and 0% indicates maximum error. Each error is scored based on its percentile ranking among all dives in the dataset, and an overall score is calculated by aggregating these individual aspect scores through uniform weighted averaging. Matsuyama et al. [60] took a different IRIS approach by explicitly predicting subscores for subactions using clear supervision from rubric data. This explicit, fine-grained assessment method enables detailed, robust evaluations, improving the model’s generalization and adaptability across diverse actions.

Both strategies offer distinct strengths and limitations for AQA applications. Uncertainty modeling [61], [62], [63] enhances robustness to noisy labels by predicting a range of plausible scores rather than a single output. However, its reliance on label distribution assumptions and difficulty generalizing from small datasets limit its versatility. Subaction assessment [55], [104] provides fine-grained insights by breaking down actions into smaller components, facilitating the identification of strengths and weaknesses. Yet, its reliance on scarce subaction labels often necessitates potentially unreliable pseudo-labels. The choice between these methods depends on whether the application prioritizes robust score predictions or detailed performance analysis. Ultimately, the choice between them depends on the specific requirements of the AQA application.

Contrastive Assessment. These approaches [25], [53], [57], [58], [147] focus on learning relative differences between actions, using techniques like contrastive learning to compare pairs of actions based on their quality. In Fig. 6, this approach usually employs a Siamese network to learn the difference between the target and the reference actions. This allows the model to capture finer details in performance and distinguish between similar actions with varying degrees of quality. Contrastive assessment, which originates from

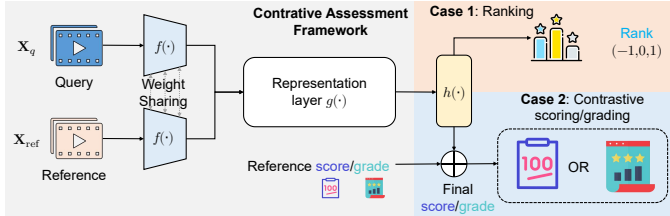


Fig. 6: Pairwise contrastive AQA framework. Different ranking (Case 1), contrastive scoring, or ranking (Case 2) requires the reference’s label.

ranking-aware methods [15], [40], [140], [141], has become prevalent in scoring and ranking [25], [57], [58] due to its effectiveness in distinguishing varying levels of performance.

Rank-aware methods [15], [40], [41], [69], [140], [141] focus on comparing pairs of actions to determine their relative quality, rather than predicting absolute scores. By assigning videos a relative skill score for a given task, they predict a ranking across a set of videos. This approach offers several advantages. First, it mitigates the challenge of scarcity and the high cost of obtaining true ground truth labels [15] by emphasizing relative differences over absolute annotations. Second, ranking-based methods are well-suited for predicting fine-grained scores, as they can more effectively capture subtle variations in action quality, unlike grade-based methods that may group varying skill levels into broad categories [40]. Due to these benefits, ranking approaches have been widely adopted across various domains. For instance, ranking-based assessment was first applied in surgical skill evaluation [15]. Later, Gedas et al. [141] introduced the method to assess basketball performance from a first-person perspective, enabling models to learn to evaluate players in real-world games without needing access to the specific criteria used by human evaluators. More recently, TAQRM [41] proposed a ranking framework for evaluating teaching quality, helping to identify high-quality teacher actions and improve teaching behaviors based on the rankings.

In recent years, score-based and grade-based methods have increasingly integrated pairwise contrastive learning [25], [52], [53], [57], [58], [59], [108], [147], valued for its precision in capturing fine-grained action differences. Pairwise contrastive learning enhances AQA models by enabling them to distinguish between high- and low-quality actions through subtle performance variations, thereby increasing sensitivity. Notably, Jain et al. [147] were among the first to explore this approach in scoring contexts. Expanding on this, Yu et al. [25] proposed a group-aware contrastive regression framework, introducing a tree-structured hierarchy of the relative quality score through coarse-to-fine classification and regression across smaller intervals. This framework soon became a standard in sports analysis. Li et al. [66] extended this with a pairwise learning-to-rank model, focusing on the subtle differences between videos and enforcing a consistency constraint between the extended branch and the basic regression network. More recently, Ke et al. [67] fused information from multiple visual fields to eliminate subjective noise from individual perspectives, enabling models to filter out distractions and concentrate on athlete performance. These pairwise contrastive methods face limitations due to the restricted viewpoint and zoom scale of input

videos, which can hinder their capacity to capture subtle differences essential for accurate quality scoring. To address this, Liu et al. [38] introduced a triple-stream contrastive transformer, incorporating an additional contrastive module to contrast the input video with its replay, thereby enhancing the model’s sensitivity to fine-grained distinctions.

3.2 Skeleton-Based Approach

When $M = 1$ and $\mathbf{X}^{(1)} \in \mathbb{R}^{T \times K \times C}$ represents the skeletal input, where T , J , and C denote the number of frames, the number of joints, and the joint dimensionality, respectively, Eq. (1) corresponds to skeleton-based methods [106], [135], [148], [149], [150]. Specifically, $C = 2$ indicates 2D skeletal joints, while $C = 3$ corresponds to 3D skeletal joints. These methods evaluate human movements by analyzing the motion of key skeletal joints, excluding contextual backgrounds to focus solely on action dynamics and minimizing the noise interference typical of video-based methods. Consequently, they are well-suited for human-centric AQA tasks that do not involve interactions with other objects. Similar to video-based methods, skeleton-based approaches follow three key steps: skeletal data acquisition, skeletal representation learning, and quality prediction. Given the similarity of quality prediction approaches between skeleton- and video-based methods, this section primarily focuses on the first two steps: skeletal data acquisition and representation learning.

3.2.1 Skeletal Acquisition Methods: High-quality skeletal data strongly impacts model design. Motion capture systems and depth sensors provide precise tracking, enabling models to leverage fine-grained motion features. In contrast, RGB-based data, prone to noise and inaccuracies [48], [113], necessitates robust mechanisms to address tracking errors. Tab. 5 summarizes the widely used skeletal acquisition methods in AQA. These methods derive skeletal data from different sensors: RGB cameras, depth cameras, and motion capture systems. Each sensor has unique advantages and limitations, influencing its application scope.

RGB camera-based methods [12], [80], [135], [148], [150], [151], [152], [153], [154], [155] estimate 2D or 3D poses from video feeds. While cost-effective and widely accessible, RGB methods face challenges like occlusion, depth ambiguity, and inaccuracies in pose estimation. Early methods like OpenPose [70] enabled real-time 2D joint detection, forming a foundation for tasks like sports analysis [148]. Techniques such as 2D-to-3D pose lifting [150], [152] and multi-view reconstruction [12] have improved the accuracy of 3D pose estimation from RGB data, expanding applications to areas like healthcare [153] and ergonomic assessments [80]. Recent works integrate contextual information for better robustness in rehabilitation [154] and fitness tracking [155].

Depth sensors, like Microsoft Kinect, capture 3D skeletal data directly, offering superior joint localization. These methods [77], [78], [78], [156], [157], [157] are preferred in medical care, where precision is critical. Applications include quality assessment in physiotherapy [74] and abnormality detection in clinical settings [77]. However, depth sensors are limited by environmental settings and higher costs. Combining RGB and depth modalities (RGB-D) leverages both strengths, improving pose estimation accuracy and robustness. RGB-D systems are particularly useful in

TABLE 5
Statistics of popular skeleton acquisition techniques in AQA.

Data Acquisition	Input	Output	Typical Works
OpenPose [70]	Image	2D Joints	[135], [148], [151], [156]
MediaPipe [71]	Image	2D Joints	[154], [155]
ViTPose [72]	Image	2D Joints	[150]
CPM [158]	Image	2D Joints	[152]
MMPose [159]	Image	3D Joints	[149]
LTHP [160]	Multi-view Images	3D Joints	[161]
MotioAGF [162]	2D Joints	3D Joints	[150]
PosePrior [163]	2D Joints	3D Joints	[152]
VideoPose3D [164]	Video	3D Joints	[80], [106], [153]
MubyNet [165]	Image	3D Pose & Shape	[12]
Depth Sensors (e.g., Kinect)	Depth	3D Joints	[11], [73], [74], [75], [76], [77], [78], [157], [166], [167], [168]
Marker-Based MoCap	Human Body	3D joints	[73], [77]

complex scenarios where depth data compensates for occlusion in RGB feeds, and RGB adds contextual cues to depth data. This synergy supports AQA applications like advanced rehabilitation systems.

Optical motion capture systems (MoCap), such as Qualisys, used for the Taijiquan dataset [73], and Vicon, utilized for the fitness dataset [77], are excellent in obtaining skeletal data. They show exceptional accuracy in tracking joint positions in both static and dynamic scenarios. However, their application is constrained by several limitations, including low flexibility as multiple cameras must be installed before capturing, high cost, and reduced participant comfort since markers must be worn during the capturing process. These factors restrict their use in controlled laboratory environments with specific setup requirements.

Discussion. These methods each offer unique advantages and limitations. RGB cameras are affordable and versatile but struggle with occlusions and lack depth information. Depth sensors offer precise 3D skeletal tracking for applications like rehabilitation but are costly and sensitive to environmental constraints. Optical motion capture systems provide unmatched accuracy but are expensive, require complex setups, and are confined to controlled environments. The choice depends on balancing precision and cost.

3.2.2 Skeletal Representation Learning Methods: Unlike video-based representation learning, which focuses on pixel-based features from raw images or frames, skeletal representation learning directly works with abstract body joint coordinates and their dynamic interactions over time. The complexity of joint relationships makes skeletal representation learning distinct, as it emphasizes the spatial and temporal dependencies between body parts. This section first reviews typical feature representation methods and then introduces robust mechanisms for enhanced AQA.

Basic Learning Methods. These methods have evolved from handcrafted approaches to more advanced deep learning techniques. Handcrafted methods [39], [148] relied on predefined features and traditional machine learning models, such as DCT features and an SVM classifier for origami skill assessment [39], and self-similarity descriptors combined with SVM classifiers for scoring [148]. However, these approaches struggled to capture complex, high-dimensional patterns in skeletal data and were limited in terms of scalability and generalization. With the rise of deep learn-

ing, models like CNNs, LSTMs, GCNs, and Transformers have gained significant attention. Among these, GCN-based methods [74], [75], [76], [77], [78], [157], [166], [167] stand out for their ability to effectively model the human skeleton, leveraging its natural graph representation to capture spatial dependencies between joints more efficiently than non-GCN-based approaches [3], [169]. Modern GCN-based techniques represent body joints as graph nodes and their spatial-temporal connections as edges, enabling dynamic skeletal data modeling that significantly improves AQA performance. Initially, GCNs were limited to spatial modeling, but the introduction of ST-GCN [79] addressed the growing need for spatial-temporal processing by incorporating temporal convolution. Originally developed for action recognition, ST-GCNs have since been widely applied in skeleton-based AQA tasks.

Robust Learning Mechanisms. In practice, the performance of these networks often depends on more than architectural innovations. We identify three robust learning mechanisms for boosting AQA performance: leveraging hierarchical body part priors, robust temporal modeling, integrating multiple input forms, and self-supervised learning.

One kind of advancement in skeleton-based AQA leverages hierarchical body part semantics to improve AQA performance [73], [78], [135], [166]. For instance, Liao et al. [78] proposed a framework that analyzes joint displacements through sub-networks, processing body parts individually and then integrating features. Similarly, Wang et al. [73] implemented a partially connected LSTM to emphasize skeletal relations while reducing the complexity of joint movements, while Deb et al. [166] leveraged self-attention to highlight critical joints, accommodating variable-length exercises. MS-GCN [135] utilized a multi-scale GCN to model joint and body-part relationships for accurate AQA.

Further refinements involve integrating multiple input forms to enhance skeletal representation robustness. EGCN [74] leveraged the ensemble concept to capture both positional and orientational data, and later was extended as EGCN++ [75], combining data and model fusion strategies to capture complex skeletal dynamics. In addition, multi-task frameworks have also emerged. For example, 2T-GCN [77] integrated abnormality detection and quality assessment for enhanced Alzheimer’s monitoring. Li et al. [76] expanded on this by introducing a siamese network that compares test actions to standard actions, blending classification with assessment. Similarly, Yao et al. [167] applied contrastive learning, allowing fine differentiation in movement quality through multi-task performance metrics.

Finally, self-supervised learning has contributed to model robustness and generalization. Nekoui et al. [170] proposed a two-stage approach where a non-expert network first learns basic motion patterns before an expert network evaluates domain-specific actions. Du et al. [157] further improved robustness by incorporating self-supervised regularization, enabling the network to learn consistent action patterns independently. Together, these methods highlight the continuous refinement of AQA systems by leveraging in-depth skeletal data and advanced learning strategies.

Discussion. While GCN-based models effectively capture spatial-temporal dependencies, challenges remain in generalization, handling variable-length sequences, and dis-

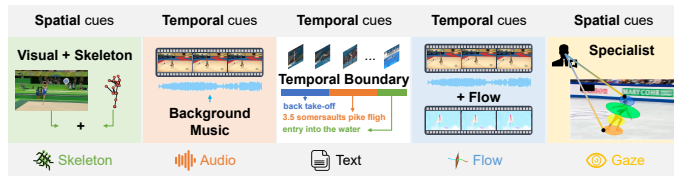


Fig. 7: Illustration of typical multi-modal AQA methods.

tinguishing subtle movement differences. Recent advancements, such as hierarchical semantics, multi-task frameworks, and self-supervised learning, enhance robustness but often increase complexity and computational demands. Future efforts should focus on lightweight, interpretable, and adaptable models for real-world, online applications.

3.3 Multi-Modality Approach

When $M > 1$, Eq. (1) corresponds to the multi-modal AQA methods [81], [82], [83]. Fig. 7 illustrates its core concept of leveraging diverse data modalities to build a comprehensive understanding of human actions. This approach addresses limitations inherent to uni-modal methods, such as the sensitivity of RGB data to lighting or the susceptibility of depth data to interference. Leveraging multi-modal inputs can capture a broader range of details, enhancing both robustness and accuracy. This makes them particularly valuable in applications like sports analysis [26], [27], [29], [81], [82], [83], [84], [85] and medical rehabilitation [89], [90], [171], [172], where detailed, precise movement assessments are crucial. In this section, we review multi-modality AQA methods categorized by the different assisted modalities utilized in their frameworks. Each modality, whether it be audio, text, video, or sensor data, offers unique advantages and insights that enhance the assessment process.

3.3.1 Audio-Assisted Methods: Audio can significantly enhance AQA by providing temporal cues and rhythmic patterns that complement visual data [29], [81], [82]. For example, in figure skating, audio captures changes in pace and flow that align with movement quality. Skating-Mixer [81] combines audio-visual inputs using a memory recurrent unit to capture long-term dependencies, addressing the rapid movement changes in skating performances. Similarly, Zhong et al. [82] propose a contrastive self-supervised approach for dance assessment, mapping dance motions, and music onto a shared latent space, which highlights the synchrony between audio and movement. PAMFN [29] integrates audio with RGB and optical flow in multiple stages, where modality-specific and mixed-modality branches progressively aggregate information. These audio-assisted frameworks capture rhythmic alignment, improving the accuracy and depth of performance evaluations.

3.3.2 Text-Assisted Methods: Text-assisted methods [26], [27], [28], [35], [83], [84], [85], [97] enhance AQA by integrating textual information with visual data, enabling richer contextual understanding. For example, NAE-AQA [27] introduced a prompt-guided multimodal interaction framework that utilizes transformers to facilitate interactions between text prompts and video content, effectively transforming score regression tasks into video-text matching tasks. VLAKL [26] addresses the limitations of coarse action

segmentation by embedding specialized terminology into multi-level representations through a multi-grained alignment framework. Its semantic-aware collaborative attention helps maintain textual knowledge across modalities. SGN [84] employs a teacher-student model with attention mechanisms, enabling adaptive knowledge transfer from semantic to visual domains and enhancing the representation of high-level semantics in sports video analysis. ZEAL [83] introduces a surgical skill assessment method leveraging zero-shot learning with text prompts for tool segmentation. By integrating segmentation masks with LSTM networks, ZEAL effectively captures critical features for precise evaluations. These text-assisted methods enhance AQA by leveraging semantic spatial and temporal cues to provide a richer contextual understanding.

3.3.3 Video-Skeleton Methods: Video-skeleton methods [64], [86], [87], [88], [175] integrate visual data with joint skeletal information, enhancing performance evaluation by capturing both spatial structures and temporal dynamics. For example, Zahan et al. [86] emphasize the importance of modeling long sequences in sports videos, introducing the AGF-Olympics dataset to address the limitations of existing benchmarks and proposing a discriminative attention module (DNLA) for improved feature representation. 2M-AF [87] further enhances assessment accuracy with RGB and skeleton streams. It includes a preference fusion module to optimize feature integration, thus overcoming the constraints of relying solely on the RGB modality. More recently, Dong et al. [88] introduce the LucidAction dataset, including multi-view RGB video and 2D/3D pose sequences, and adapt several uni-modal AQA architectures for comprehensive action quality analysis. These video-skeleton methods boost performance by integrating complementary visual and skeletal features, enabling robust assessments across diverse action quality scenarios.

3.3.4 Others-Assisted Methods: Other multi-modal AQA methods [89], [90], [91], [171], [172] enhance AQA through diverse sensor integrations, such as flow, gaze, and kinematic data. For instance, Nagai et al. [171] develop the multimodal in-the-wild MMW-AQA dataset for freestyle windsurfing, incorporating video, IMU, and GPS data to enable a comprehensive assessment of complex 3D actions from varied viewpoints, supported by a transformer-based fusion module for effective multimodalization of existing deep neural network models. Hirosawa et al. [172] innovate by analyzing the gaze patterns of figure skating judges and skaters, developing a predictive model for jump performance that utilizes the gaze locations of specialists alongside kinematic features to enhance prediction accuracy. Additionally, Kim et al. [90] address the challenges of fine-grained task execution assessments by employing both RGB and optical flow data, utilizing a novel cross-attention module for modality fusion to effectively capture the correlation between the two data types. Huang et al. [91] introduce a novel skill assessment dataset featuring gaze data alongside corresponding exo-view demonstration videos. They propose a cross-view referenced skill assessment framework leveraging triplet loss and a relation network to align information across modalities effectively. These multi-modal methods highlight the potential of integrating diverse data sources to enhance the AQA performance.

TABLE 6

Overview of popular AQA datasets, including modality, domain, number of classes, sample size, average frames, annotations, and access URLs. Datasets span sports, skill assessment, and medical care, with diverse modalities such as video, 2D/3D skeletons, and audio.

Dataset	Year	Modality	Domain	# Class	# Samples	# Average Frames	Annotations	URL
MIT Olympic [113]	2014	Video 2D Skeleton	Sports	2	309	Dive: 150 Figure Skate: 4200	Score	↗
UNLV Olympic [98]	2017	Video	Sports	3	717	Dive: 150 Figure Skate: 4200 Vault: 75	Score	↗
AQA-7 [92]	2019	Video	Sports	7	1189	Dive: 97 105 156 Vault: 87 Big Air: 122 132 Trampoline: 634	Score	↗
MTL-AQA [37]	2019	Video	Sports	16	1412	96	Score	↗
Fis-V [7]	2019	Video	Sports	1	500	4300	TES PCS	↗
RG [94]	2020	Video	Sports	1	250	2375	Difficulty Execution	↗
FineDiving [57]	2022	Video	Sports	52	3000	105	Total Step Score	↗
FS1000 [81]	2023	Video Audio	Sports	7	1604	5000	TES PCS detailed PCS	↗
FineFS [64]	2023	Video 2D/3D Skeleton	Sports	4	1167	5000	detailed Score Subaction Class Segmentation	↗
LOGO [95]	2023	Video	Sports	12	200	5100	Action Class Formation Score	↗
GAIA [173]	2024	Video (AI Gen.)	Multi-Domain	510	9180	70	Subject Completeness Interaction	↗
JIGSAWS [93]	2014	Video	Skill Assessment	3	103	–	Surgemes Class Rating	↗
EPIC-Skills [40]	2018	Video	Skill Assessment	7	216	–	Relative Rank	↗
BEST [140]	2019	Video	Skill Assessment	5	500	6400	Relative Rank	↗
PISA [14]	2021	Video Audio	Skill Assessment	1	992	160	Skill Level Difficulty	↗
TAQR [41]	2024	Video	Skill Assessment	4	300	488	Relative Rank	↗
EgoExoLearn [91]	2024	Video	Skill Assessment	8	3304	250	Relative Rank	↗
UI-PRMD [174]	2018	3D Skeleton Joint Pos. & Ori.	Medical Care	10	1326	–	Binary Class	↗
KIMORE [11]	2019	Video, 3D Skeleton Joint Pos. & Ori.	Medical Care	5	1560	–	Score	↗
EHE [77]	2021	3D Skeleton Joint Pos. & Ori.	Medical Care	6	869	–	Binary Class	↗
FineRehab [168]	2024	Video, 3D Skeleton Joint Pos. & Ori.	Medical Care	16	4215	–	Score	↗

3.3.5 Discussion: Recent years have seen a notable rise (see Fig. 1) in multi-modal AQA methods [26], [29], [81], [91], which provide a comprehensive perspective on AQA. While these methods offer enhanced robustness, they face practical challenges, including the high cost of acquiring and processing full modalities during inference. Additionally, reliance on all modalities may limit applicability in real-world scenarios with constrained resources or incomplete modalities (see Sec. 6 for further discussions).

4 DATASET AND BENCHMARK

This section outlines the prominent public datasets and presents a unified benchmark for consistent comparison.

4.1 Current Trend of Datasets

We have summarized the public datasets for AQA, as shown in Tab. 6. These datasets vary widely in various dimensions, serving applications in sports, skill assessment, and medical care. Sports datasets, like AQA-7 [92] and FineDiving [57], capture activities such as diving and gymnastics, often

sourced from Olympic broadcasts, with detailed scoring annotations to assess nuanced movement dynamics. Skill assessment datasets, such as JIGSAWS [93] and PISA [14], focus on controlled tasks like surgery or piano performance, using expert-provided rankings to evaluate technical proficiency. Medical care datasets, including UI-PRMD [174] and FineRehab [168], leverage skeletal data to objectively assess movement quality in therapeutic exercises. Below, we discuss these datasets across three key trends: growth in multi-modal and fine-grained annotations, increasing large-scale data availability, and emerging application domains.

A key trend in AQA datasets is the growing adoption of multi-modality and fine-grained annotations, which enhance the interpretability and precision of AQA models. For example, sports datasets such as FineDiving [57] and FineFS [64] include step-level annotations and subaction classes, enabling detailed action analysis. Similarly, skill assessment datasets like PISA [14] and EgoExoLearn [91] integrate video and audio modalities to capture subtle skill differences. In medical care, datasets such as FineRehab [168] utilize 3D skeleton data and joint orientation informa-

TABLE 7

Results of our video-based AQA benchmark. The training time unit is in hours. The average SRCC is calculated using Fisher-z transformation to ensure comparability across datasets. The best results are presented in **bold**, while the second-best results are underlined. These results reflect the performance of the methods based on our implementation using their official code.

Method	Publisher	MTL-AQA [37]				AQA-7 ^{Average} [92]				FineDiving [57]				RG ^{Average} [94]				Fis-V ^{Average} [7]				LOGO [95]			
		SRCC	MSE	rMSE	Time	SRCC	MSE	rMSE	Time	SRCC	MSE	rMSE	Time	SRCC	MSE	rMSE	Time	SRCC	MSE	rMSE	Time	SRCC	MSE	rMSE	Time
MUSDL [61]	CVPR'20	0.9350	39.7753	0.3642	11.32	<u>0.8291</u>	268.2845	3.0782	1.57	0.8891	48.9616	0.4492	7.72	0.4182	12.3617	4.4668	0.01	0.0000	481.6830	41.6013	0.02	0.7044	34.9489	3.6828	0.04
CoRe [25]	ICCV'21	0.9519	32.9234	0.3015	46.81	0.8106	22.1156	2.8686	4.54	0.9406	26.7377	<u>0.2453</u>	26.62	0.7038	6.6751	2.3689	0.06	0.7068	16.4629	<u>1.7725</u>	0.20	0.5968	47.2615	4.9803	0.08
GDLT [36]	CVPR'22	0.9395	43.5769	0.3990	10.84	0.8164	<u>214.4547</u>	<u>2.4393</u>	1.57	0.9351	29.2547	0.2684	8.84	<u>0.7486</u>	6.8529	<u>2.4856</u>	0.02	0.7550	19.4951	1.9746	0.04	0.6608	33.7699	3.5586	0.04
HGCN [24]	TCSVT'23	<u>0.9522</u>	30.7432	0.2815	14.79	0.8450	235.3630	2.7660	1.54	0.9381	26.3895	0.2421	9.14	0.7329	7.2040	2.6379	0.02	0.7265	17.7051	1.8885	0.03	0.6709	62.2947	6.5644	0.03
DAE [63]	NCAA'24	0.9497	31.3355	0.2869	<u>11.11</u>	0.7907	298.5182	3.4030	1.59	0.9356	27.1739	0.2493	<u>8.58</u>	0.7390	6.9272	2.5971	0.02	0.7422	16.7924	1.7965	<u>0.03</u>	0.6701	<u>33.8434</u>	<u>3.5663</u>	0.02
T ² CR [67]	INFS'24	0.9529	29.8640	0.2735	49.62	0.7908	303.5029	3.4776	4.99	<u>0.9382</u>	27.2114	0.2497	30.56	0.6581	7.0013	2.5215	0.28	<u>0.7606</u>	1.4188	1.4429	1.09	0.6074	40.3653	4.2536	0.29
CoFinAI [65]	IJCAI'24	0.9461	37.7907	0.3461	14.80	0.8194	250.1018	2.7787	<u>1.57</u>	0.9317	36.4681	8.64	0.8049	8.7432	3.2509	0.06	0.7972	21.8519	2.3514	0.08	<u>0.6979</u>	38.1411	4.0192	0.04	
		Diving ^{AQA-7} [92]				Gym Vault ^{AQA-7} [92]				BigSki. ^{AQA-7} [92]				BigSnow. ^{AQA-7} [92]				Sync. 3m ^{AQA-7} [92]				Sync. 10m ^{AQA-7} [92]			
MUSDL [61]	CVPR'20	0.8738	129.5963	1.2960	3.21	0.7300	133.8101	2.1927	1.44	0.5369	729.6780	8.4625	1.44	0.7109	366.3390	3.6634	1.64	0.9205	126.1327	1.5508	0.85	0.9416	124.1512	1.3039	0.86
CoRe [25]	ICCV'21	0.8589	7.8716	0.8746	8.13	0.7297	19.9152	3.6261	4.34	0.6023	37.6885	4.8566	4.35	0.5728	37.6983	4.1887	5.20	0.9065	11.0951	1.5158	2.62	0.9353	18.4246	2.1500	2.60
GDLT [36]	CVPR'22	0.8735	78.9092	0.7891	3.19	0.7806	143.5258	2.3519	1.42	<u>0.6380</u>	<u>376.0729</u>	4.3616	1.46	0.6122	417.0589	4.1706	1.65	0.9078	64.1058	0.7882	0.85	0.9049	207.0555	2.1746	0.86
HGCN [24]	TCSVT'23	0.8871	101.4813	1.0148	3.16	0.7725	220.5605	3.6143	1.36	0.6701	483.7507	5.6104	1.40	0.6487	369.5956	3.6960	1.59	0.9174	96.7002	1.1890	0.86	0.9507	140.0894	1.4713	0.85
DAE [63]	NCAA'24	0.8440	85.3052	<u>0.8531</u>	3.20	0.7514	141.5409	2.3194	<u>1.42</u>	0.5367	597.1253	6.9252	1.49	0.5157	458.1914	4.5819	1.68	0.9254	219.1645	2.6947	0.87	0.8923	289.7821	3.0434	0.87
T ² CR [67]	INFS'24	0.8334	96.7862	0.9679	9.13	0.7585	187.0455	3.0651	4.93	0.5887	482.7082	5.8593	5.03	0.4790	546.7196	5.4672	5.55	0.9087	242.4116	2.9805	2.58	0.9109	265.3465	2.7868	2.71
CoFinAI [65]	IJCAI'24	0.8652	150.5001	1.5050	3.17	0.7685	<u>126.4775</u>	2.0726	1.43	0.6119	394.2921	<u>4.5729</u>	1.45	0.5990	539.6546	5.3965	1.64	0.9073	<u>46.2191</u>	0.5683	0.85	0.9334	243.4674	2.5770	0.87
		Ball ^{RG} [94]				Clubs ^{RG} [94]				Hoop ^{RG} [94]				Ribbon ^{RG} [94]				TES ^{Fis-V} [7]				PCS ^{Fis-V} [7]			
MUSDL [61]	CVPR'20	0.3414	14.3111	3.8222	0.01	0.4746	9.2043	4.3180	0.01	0.4919	11.6340	4.3788	0.01	0.3555	14.2974	5.3484	0.01	0.0000	932.2650	78.2344	0.02	0.0000	31.1011	4.9682	0.02
CoRe [25]	ICCV'21	0.6128	9.1890	2.4542	0.06	<u>0.7492</u>	4.8258	2.2639	0.06	0.7494	5.2598	1.9797	0.06	0.6875	7.4259	2.7779	0.06	0.6399	22.6156	1.8979	0.20	0.7631	10.3102	1.6470	0.20
GDLT [36]	CVPR'22	<u>0.7549</u>	8.9492	2.3901	0.02	0.6886	6.6412	3.1156	0.02	0.7202	6.3356	2.3846	0.02	0.8150	5.4857	2.0521	0.02	0.6670	30.0593	2.5225	0.04	<u>0.8223</u>	8.9309	1.4267	0.04
HGCN [24]	TCSVT'23	0.6969	7.6504	2.0432	0.02	0.7177	6.0215	2.8249	0.02	0.7538	7.9099	2.9771	0.02	0.7589	7.2342	2.7062	0.02	0.6637	24.7891	2.0803	0.03	0.7792	10.6211	1.6967	0.03
DAE [63]	NCAA'24	0.7425	5.3578	1.4310	0.02	0.7425	6.1528	2.8865	0.02	0.7380	5.0582	1.9038	0.02	0.7328	11.1399	4.1672	0.02	0.6781	23.3684	1.9610	0.03	0.7951	10.2164	<u>1.6320</u>	0.03
T ² CR [67]	INFS'24	0.5368	8.6685	2.3152	0.28	0.7301	5.4878	2.5745	0.28	0.6447	6.7768	2.5506	0.28	0.6979	7.0722	2.6456	0.28	0.8089	1.7413	1.1510	1.14	0.7020	1.0964	1.7348	1.05
CoFinAI [65]	IJCAI'24	0.8070	5.0843	1.3579	0.06	0.8022	4.4294	2.0780	0.08	0.8004	19.1641	7.2129	0.06	<u>0.8098</u>	<u>6.2952</u>	<u>2.3549</u>	0.04	<u>0.7109</u>	30.0518	2.5219	0.08	0.8598	13.6520	2.1808	0.08

tion, supporting detailed evaluations of patient movement quality. These advancements in annotations and modalities facilitate the development of more robust AQA methods.

Another important trend is the increasing availability of large-scale datasets, which enable comprehensive evaluations across various domains. Notable examples include the GAIA dataset [173], which contains 9180 samples across 510 classes, representing a significant milestone in dataset size and diversity for AI-generated content. In the sports domain, datasets like FS1000 [81] provide over 1600 samples with detailed program component scores for figure skating. Similarly, skill assessment datasets such as EgoExoLearn [91] contain more than 3000 samples, allowing for robust evaluations of complex human activities. These large datasets provide a strong foundation for developing and benchmarking AQA models.

Finally, AQA research is expanding into new and emerging application domains. The GAIA dataset [173] exemplifies the rise of AI-generated video content, offering annotations for subject completeness and interaction. In the skill assessment domain, datasets like TAQR [41] and EgoExoLearn [91] focus on evaluating teaching techniques and interaction quality, broadening the practical applications of AQA. In medical care, datasets such as FineRehab [168] provide objective metrics for movement quality in rehabilitation tasks, supporting therapeutic applications. This diversification of domains demonstrates the increasing relevance of AQA methods in addressing real-world challenges. These developments pave the way for innovative methods capable of addressing challenges across various application areas.

4.2 A Unified AQA Benchmark

In previous studies, AQA methods have typically been evaluated on a narrow selection of benchmark datasets. In addition, differences in evaluation metrics and experimental setups across these works have made it challenging to achieve fair comparisons and a comprehensive assessment of various methods. To address this critical issue, this study primarily focuses on constructing a benchmark

for video-based AQA, which is the most widely studied and established branch of AQA. In contrast, multi-modal and skeleton-based approaches, although promising, are less accessible due to the limited availability of open-source codes. This scarcity makes it difficult to create a unified framework for these methods. By concentrating on video-based AQA, we aim to address the pressing need for a standardized benchmark in this mature and widely explored area, laying a solid foundation that can later be extended to other modalities as more resources become available.

4.2.1 Experimental Setting: Our experimental setup encompasses six representative benchmark datasets, seven state-of-the-art baseline methods, and seven key evaluation metrics, including correlation, precision, and computation measures. To ensure a fair comparison, we adopt a consistent configuration across all experiments.

Benchmark Datasets. The selected datasets include both long-term and short-term benchmarks commonly used in the field. For long-term evaluations, we used datasets such as Fis-V [7], RG [94], and LOGO [95]. For short-term evaluations, we utilized datasets including MTL-AQA [37], FineDiving [57], and AQA-7 [92]. This combination ensures a balanced assessment of methods across varying temporal scales and domain complexities.

Benchmark Methods. The baseline methods were chosen based on three criteria. First, they have publicly available source code validated by the research community. Second, they represent state-of-the-art techniques across different paradigms. Third, they demonstrate adaptability to multiple domains, especially those constrained by limited annotations. Specifically, we included the uncertainty-aware MUSDL [61] and DAE [63], the contrastive regression-based CoRe [25] and T²CR [67], the transformer-based GDLT [36] and CoFinAI [65], and the GCN-based HGCN [24]. Note that for MUSDL on the MTL-AQA dataset with detailed judge scores, we use MUSDL, while for the other datasets, we use USDL. These methods collectively provide diverse benchmarks for comprehensive comparison and evaluation.

Evaluation Metrics. For evaluation, we used widely

accepted metrics, including the correlation metric (SRCC) for ranking consistency, absolute error for precision (MSE), and relative error (rMSE) for comparative accuracy. Beyond these traditional metrics, we also measured computational performance, including training time, model size (parameters), inference time, and computation complexity. This holistic evaluation framework allows for a nuanced analysis of trade-offs between accuracy and efficiency.

Implementation Details. The experimental setting primarily followed the official settings of the baseline methods to ensure fair comparisons. For datasets without officially provided configurations, we applied a unified setup across all methods. Experiments were conducted using a single NVIDIA RTX 3090 GPU. The default settings included a maximum of 100 training epochs, an Adam optimizer with a weight decay of 0.0001, and a learning rate of 0.0001. Batch sizes were set to 2 for training and 1 for testing. For the backbone, we used the widely adopted I3D model [46] pre-trained on the Kinetics 400 dataset. For the long-term datasets RG and Fis-V, we used the officially released features extracted with the VST backbone [47]. By maintaining consistency in settings and ensuring fair comparisons, this experimental design provides a robust evaluation of the selected methods across diverse datasets and scenarios.

4.2.2 Assessment Performance: Tab. 7 presents a detailed performance comparison of seven representative AQA methods across six benchmark datasets spanning about 20 categories. We employ three assessment metrics, SRCC, MSE, and rMSE, to comprehensively evaluate both ranking and prediction accuracy. The results are based on our implementation using the official code, ensuring that performance differences reflect the intrinsic characteristics of the methods rather than implementation variations.

Transformer-based methods have demonstrated robustness, particularly in long-term AQA tasks involving complex relationships. Specifically, CoFInAI [65] shows significant performance advantages on long-term datasets such as RG, Fis-V, and LOGO. For instance, in the RG dataset, CoFInAI achieves an SRCC of 0.8049, significantly outperforming the second-best GDLT [36], which scores 0.7486, with an improvement of 7.5%. Additionally, CoFInAI performs similarly well on other long-term datasets, showcasing its effectiveness in handling complex and nonlinear relationships. However, USDL/MUSDL [61] exhibits instability, particularly on the Fis-V dataset, where it fails to converge. This instability can be attributed to the challenging nature of the Fis-V dataset, which likely introduces noise and variability that USDL struggles to handle. Furthermore, the Transformer-based method’s design may make it more unstable when faced with data containing significant noise or complex, long-term dependencies.

Contrastive regression-based methods [25], [67], achieve the highest SRCC scores on large-scale datasets like MTL-AQA and FineDiving. However, on smaller-scale datasets, their performance is less stable. For example, on the LOGO dataset, CoRe [25] and T²CR [67] obtain SRCC scores of 0.5968 and 0.6074, respectively, falling behind USDL, which scores 0.7044, with a performance gap of 14.6%. This instability arises because contrastive regression methods rely heavily on large datasets to effectively learn and generalize. In smaller datasets, the limited data points lead to over-

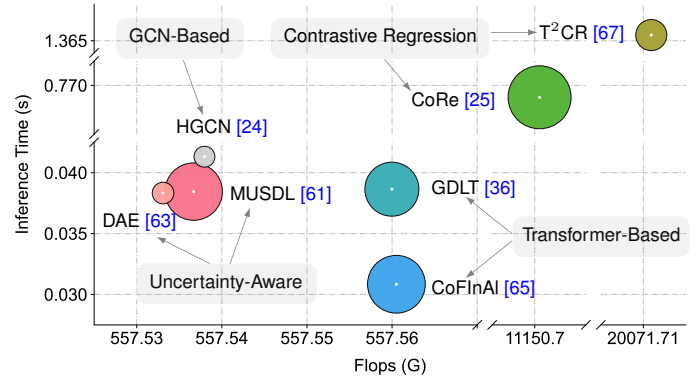


Fig. 8: Computational performance comparison with selected baselines under the identical device settings on the MTL-AQA dataset. The x-axis represents the FLOPs, the y-axis indicates the inference time, and the bubble size corresponds to the number of parameters.

fitting and poor generalization, especially when noise is present and the sample size is insufficient for stable model training. The uncertainty-aware DAE [63] does not exhibit strong performance in this study. Finally, the GCN-based HGNC [24] shows notable advantages. HGNC achieves the best correlation performance on the AQA-7 dataset and the best precision performance (in terms of MSE and rMSE) on FineDiving. By leveraging graph structures to model local and global feature relationships, HGNC is able to extract more robust feature representations, which contributes to its superior performance on these tasks.

4.2.3 Computational Performance: When analyzing the computational performance of the AQA methods, based on the provided training time (see Tab. 7), FLOPs, parameters, and inference time (see Fig. 8), we observe distinct differences in computation efficiency across the methods. The computational performance in Fig. 8 reflects statistics obtained from the MTL-AQA dataset.

The contrastive regression methods [25], [67] have the longest training and inference times. For example, in the MTL-AQA dataset, CoRe [25] and T²CR [67] require 46 and 49 hours for training, respectively, while GDLT [36] only takes 10 hours. This is primarily because these methods need additional time to compute exemplars, and during inference, the ensemble strategy often selects multiple exemplars to improve robustness. T²CR [67] is particularly computationally intensive, as it uses two different time scales for the same input, effectively doubling the computation. In contrast, the direct regression methods [24], [61], [65] have relatively similar training and inference times, with CoFInAI [65] having the shortest inference time of 0.03s, while T²CR takes about 1.4s. Regarding parameter count, HGNC [24] and DAE [63] have the fewest parameters, with 12.56M and 12.58M, respectively, compared to the Backbone model’s 12.29M. In terms of computational complexity, DAE [63] requires the least at 557.53G, while T²CR [67] exceeds this by more than 30 times.

4.2.4 Experimental Observations: As shown in Tab. 7 and Fig. 8, the observations from our benchmark further reinforce the lack of a clear winner among existing AQA methods. By systematically evaluating diverse approaches across various datasets and domains, our benchmark provides critical insights into the strengths and limitations of

each method. This underscores the domain-specific nature of AQA and highlights the pressing need for approaches capable of generalizing across different scenarios. The findings not only confirm the current limitations in achieving a universal AQA solution but also pave the way for future research to focus on enhancing computational and cross-domain performance, such as through zero-shot or few-shot learning and leveraging foundation models.

5 TASK-SPECIFIC APPLICATIONS

Beyond common setup in Secs. 2 and 3, this section highlights three task-specific applications that have received moderate attention for addressing real-world challenges.

5.1 Semi-Supervised AQA

The *scarcity of labeled data* poses a significant challenge to improving AQA performance, primarily due to the high level of expertise required and the substantial costs associated with annotation. Semi-supervised AQA [30], [31], [52] addresses this issue by leveraging both labeled and unlabeled data. By reducing reliance on extensive labeled datasets, these methods utilize abundant unlabeled data to enhance model performance through techniques such as self-training, consistency regularization, and pseudo-labeling. S⁴AQA [30] was the first semi-supervised approach for AQA, leveraging a masked segment recovery module to exploit temporal patterns from unlabeled videos, enabling effective assessment with limited labeled data. Yun et al. [31] introduced a teacher-reference-student (TRS-AQA) architecture, where the teacher and reference networks generate pseudo-labels for unlabeled data to guide the student network, enhancing performance with both labeled and unlabeled data. In addition, domain transfer techniques address this challenge by leveraging knowledge from related domains to enhance performance in the target domain. AdaST [96] introduced novel constraints to ensure that transferred assessment skills do not degrade accuracy and instead provide complementary information, promoting the transfer of effective and non-redundant assessment skills. These approaches improve generalization and mitigate the costs and expertise barriers of manual annotation.

5.2 Continual AQA

Non-stationary variations in AQA pose significant challenges due to fluctuations in user performance, environmental factors, and recording conditions. These dynamic changes can severely impact the effectiveness of AQA models, as they often struggle to adapt to evolving patterns in how actions are performed, recorded, or assessed over time. To tackle this issue, continual AQA [32], [33], [34] has emerged as a promising solution. By leveraging continual learning techniques [23], [176], this approach enables models to dynamically adapt to new information and shifting data distributions, ensuring improved robustness and long-term performance. PECOP [34] focused on continual training strategies that minimize domain shifts, which is crucial for maintaining model performance when data characteristics change. Li et al. [33] explored facilitating continual learning across different action categories, allowing AQA

systems to update their knowledge base as new action types are introduced, ensuring broader applicability. Meanwhile, MAGR [32] proposed a manifold projector and a graph regularizer to address the misalignment due to backbone updates, ensuring sustained accuracy in memory stability and protecting user privacy. These approaches enhance the system to manage non-stationary variations, maintaining its robustness in real-world applications.

5.3 Interpretable AQA

The *non-interpretability of feedback* poses a significant challenge to the practical utility of AQA systems. Most traditional AQA methods provide only simple numerical scores, preventing users from pinpointing specific aspects of their performance that require improvement. To address this issue, interpretable AQA aims to provide actionable insights beyond simple quality scores, enabling users to gain a deeper understanding of their performance and identify areas for improvement more effectively. One way is to provide human-readable narrative feedback [12], [27], [35], [55], [97] for improved interpretability. Aifit [12] pioneered natural language feedback by generating active or passive grammar-based instructions for trainees. NSAQA [55] enhanced this way with detailed reports tailored for sports, offering comprehensive performance insights. NAE-AQA [27] generated customized action descriptions and corrective feedback to improve user performance. Most recently, ExpertAF [97] advanced narrative outputs by providing personalized, language-based commentary that identifies specific mistakes and suggests actionable corrections. TechCoach [35] generated key point-level feedback, offering detailed insights into action quality and areas for improvement. Another way is to deliver visually interpretable outputs [12], [13], [97] for enhanced understanding. Aifit [12] provided side-by-side visual comparisons, displaying the user's errors alongside reference images demonstrating correct execution. JDM-AQA [13] incorporated animations to visualize feedback, offering clinicians a human-in-the-loop verification interface. This approach enables clinicians to assess the reliability of machine-generated scores by comparing the difference between predicted and actual motions, thereby enhancing interpretability and trust in the system. Both methods enhance AQA transparency by offering intuitive insights beyond a single numerical score.

6 DISCUSSION

This section provides an in-depth discussion of under-explored challenges and cross-directional prospects.

6.1 Under-explored Challenge

Recent advancements in AQA reveal two prominent trends. The first is the shift towards multi-modal approaches, which integrate visual, skeletal, and other sensor data to assess action quality. This trend is supported by the increasing availability of multi-modal datasets [64], [88] (see Sec. 4.1), fueling the development of more comprehensive AQA systems. The second trend focuses on the emphasis on interpretable feedback. Innovations in this area include mechanisms for generating narrative explanations [12], [27],

[35], [97] and context-aware visualizations [12], [13], [97]. These advancements enhance AQA systems by providing not only quantitative outputs but also actionable feedback that highlights specific areas for performance improvement.

However, current trends in AQA methods still face certain limitations. For multi-modal AQA approaches, the absence of key modalities can significantly undermine performance, reducing system robustness and accuracy. While interpretable feedback offers valuable insights, its credibility is not always guaranteed, presenting challenges for its application in critical domains. Furthermore, certain areas, such as AIGC-based AQA, occlusions in first-person perspectives, and adversarial vulnerabilities, remain under-explored, offering opportunities for further research.

6.2 Cross-Directional Prospect

The future of AQA research lies at the intersection of multiple disciplines, presenting opportunities to address under-explored challenges and unlock new applications.

6.2.1 Incomplete Multi-Modal Learning: Real-world data collection is often noisy or incomplete, especially in dynamic environments like sports arenas or clinical settings. However, existing multi-modal AQA methods do not account for the challenge of incomplete modalities, which can significantly impact the robustness and accuracy of the AQA system in real-world scenarios. Incorporating incomplete multi-modal learning [177] can enable AQA systems to adapt to missing data scenarios, ensuring resilience and consistent performance despite imperfect inputs.

6.2.2 Causality Learning for Enhanced Credibility: While interpretable AQA models aim to provide easy-to-understand feedback, they often fall short in explaining the reasoning behind the assigned feedback. Causality learning [178] directly addresses this gap by identifying cause-effect relationships between action components and scores. By revealing the underlying factors contributing to quality assessments, causality learning enhances the credibility and transparency of AQA systems, ensuring that feedback is not only interpretable but also justifiable.

6.2.3 AI-Generated Content (AIGC) for Data Augmentation: One critical limitation of AQA models is their dependence on limited labeled data, stemming from the labor-intensive process of acquiring high-quality annotations. AIGC [173], [179] can synthesize diverse training samples, representing varied action qualities or styles, thus improving model robustness. Moreover, AIGC-generated references can standardize evaluation benchmarks, ensuring consistency in scoring while reducing data collection costs.

6.2.4 Ego-Awareness in AQA: Ego-aware AQA [91], [180] considers the observer's perspective and contextual dynamics during action evaluation. This aligns with advances in embodied AI, which has the potential to enhance performance in dynamic, interactive environments, such as sports coaching, drone-based surveillance, and AR/VR training systems. Future research can explore leveraging embodied AI principles to develop robust, context-sensitive AQA models in more immersive and complex scenarios.

6.2.5 Adversarial Robustness in AQA: As AQA systems gain adoption, especially in competitive environments, they become targets for adversarial attacks. For instance,

slight perturbations in input data could mislead models into assigning incorrect scores. Incorporating adversarial defense mechanisms [181] ensures that models remain reliable and secure, maintaining fairness and trustworthiness.

7 CONCLUSION

This survey provides a comprehensive analysis of over 150 AQA-related papers, presents a unified benchmark, and identifies under-explored challenges and prospects in AQA. Recognizing input modality as a pivotal factor in AQA model design, we propose a hierarchical taxonomy that examines each input type and its unique characteristics, improving clarity on the evolution and interrelations across distinct approaches. The proposed unified benchmark includes a series of baselines on multiple representative datasets, comparing both accuracy and the often-overlooked computational performance. This addresses the fragmentation in evaluations and the inconsistencies in comparisons observed across existing works. Furthermore, we review task-specific applications, identify under-explored challenges, and highlight potential future directions. These include expanding AQA applications to cross-directional domains, improving interpretability, and enhancing scalability for real-world deployment. Our goal is to foster innovation and ensure the robustness and practical applicability of AQA methods across diverse scenarios.

ACKNOWLEDGMENTS

This work was supported in part by the National Natural Science Foundation of China under Grant 62272019.

REFERENCES

- [1] Y. Li, X. Chai, and X. Chen, "End-to-end learning for action quality assessment," in *PCM*, pp. 125–134, Springer, 2018.
- [2] W. Sun, Y. Hu, B. Zhang, X. Chen, C. Hao, and Y. Gao, "A novel blind action quality assessment based on multi-headed gru network and attention mechanism," in *IAIHPC*, vol. 12717, pp. 835–843, SPIE, 2023.
- [3] D. Zhang, D. Zhou, and H. Liu, "Action quality assessment for asd behaviour evaluation," in *ICMLC*, pp. 483–488, IEEE, 2023.
- [4] D. Liu, Q. Li, T. Jiang, Y. Wang, R. Miao, F. Shan, and Z. Li, "Towards unified surgical skill assessment," in *CVPR*, pp. 9522–9531, 2021.
- [5] C. K. Ingwersen, A. Xarles, A. Clapés, M. Madadi, J. N. Jensen, M. R. Hannemose, A. B. Dahl, and S. Escalera, "Video-based skill assessment for golf: Estimating golf handicap," in *International Workshop on Multimedia Content Analysis in Sports*, pp. 31–39, 2023.
- [6] A. S. Gordon, "Automated video assessment of human performance," in *AI-ED*, vol. 2, p. 10, 1995.
- [7] C. Xu, Y. Fu, B. Zhang, Z. Chen, Y.-G. Jiang, and X. Xue, "Learning to score figure skating sport videos," *IEEE TCSVT*, vol. 30, no. 12, pp. 4578–4590, 2019.
- [8] Y. Zhang, W. Xiong, and S. Mi, "Learning time-aware features for action quality assessment," *PRL*, vol. 158, pp. 104–110, 2022.
- [9] M. Nekoui, F. O. T. Cruz, and L. Cheng, "Eagle-eye: Extreme-pose action grader using detail bird's-eye view," in *WACV*, pp. 394–402, 2021.
- [10] Y. LIU, X. CHENG, and T. IKENAGA, "A hierarchical joint training based replay-guided contrastive transformer for action quality assessment of figure skating," *IEICE Transactions on Fundamentals of Electronics, Communications and Computer Sciences*, 2024.
- [11] M. Capecci, M. G. Ceravolo, F. Ferracuti, S. Iarlori, A. Monteriu, L. Romeo, and F. Verdini, "The kimore dataset: Kinematic assessment of movement and clinical scores for remote monitoring of physical rehabilitation," *TNSRE*, vol. 27, no. 7, pp. 1436–1448, 2019.

- [12] M. Fieraru, M. Zanfir, S. C. Pirlea, V. Olaru, and C. Sminchisescu, "Aifit: Automatic 3d human-interpretible feedback models for fitness training," in *CVPR*, pp. 9919–9928, 2021.
- [13] K. Zhou, R. Cai, Y. Ma, Q. Tan, X. Wang, J. Li, H. P. Shum, F. W. Li, S. Jin, and X. Liang, "A video-based augmented reality system for human-in-the-loop muscle strength assessment of juvenile dermatomyositis," *IEEE TVCG*, vol. 29, no. 5, pp. 2456–2466, 2023.
- [14] P. Parmar, J. Reddy, and B. Morris, "Piano skills assessment," in *MMSP*, pp. 1–5, IEEE, 2021.
- [15] Q. Zhang and B. Li, "Relative hidden markov models for video-based evaluation of motion skills in surgical training," *IEEE TPAMI*, vol. 37, no. 6, pp. 1206–1218, 2014.
- [16] H. Wang and C. Schmid, "Action recognition with improved trajectories," in *ICCV*, pp. 3551–3558, 2013.
- [17] P. Scovanner, S. Ali, and M. Shah, "A 3-dimensional sift descriptor and its application to action recognition," in *ACM MM*, pp. 357–360, 2007.
- [18] V. Venkataraman, P. Turaga, N. Lehrer, M. Baran, T. Rikakis, and S. Wolf, "Attractor-shape for dynamical analysis of human movement: Applications in stroke rehabilitation and action recognition," in *CVPRW*, pp. 514–520, 2013.
- [19] S. Chi, H.-g. Chi, Q. Huang, and K. Ramani, "Infocn++: Learning representation by predicting the future for online skeleton-based action recognition," *IEEE TPAMI*, 2024.
- [20] Q. Lei, J.-X. Du, H.-B. Zhang, S. Ye, and D.-S. Chen, "A survey of vision-based human action evaluation methods," *Sensors*, vol. 19, no. 19, p. 4129, 2019.
- [21] S. Wang, D. Yang, P. Zhai, Q. Yu, T. Suo, Z. Sun, K. Li, and L. Zhang, "A survey of video-based action quality assessment," in *INSAI*, pp. 1–9, IEEE, 2021.
- [22] J. Liu, H. Wang, K. Stawarz, S. Li, Y. Fu, and H. Liu, "Vision-based human action quality assessment: A systematic review," *Expert Systems with Applications*, p. 125642, 2024.
- [23] L. Wang, X. Zhang, H. Su, and J. Zhu, "A comprehensive survey of continual learning: theory, method and application," *TPAMI*, 2024.
- [24] K. Zhou, Y. Ma, H. P. Shum, and X. Liang, "Hierarchical graph convolutional networks for action quality assessment," *IEEE TCSVT*, vol. 33, no. 12, pp. 7749–7763, 2023.
- [25] X. Yu, Y. Rao, W. Zhao, J. Lu, and J. Zhou, "Group-aware contrastive regression for action quality assessment," in *ICCV*, pp. 7919–7928, 2021.
- [26] H. Xu, X. Ke, Y. Li, R. Xu, H. Wu, X. Lin, and W. Guo, "Vision-language action knowledge learning for semantic-aware action quality assessment," in *ECCV*, 2024.
- [27] S. Zhang, S. Bai, G. Chen, L. Chen, J. Lu, J. Wang, and Y. Tang, "Narrative action evaluation with prompt-guided multimodal interaction," in *CVPR*, pp. 18430–18439, 2024.
- [28] A. Majeedi, V. R. Gajjala, S. S. S. N. GNVV, and Y. Li, "Rica²: Rubric-informed, calibrated assessment of actions," *arXiv preprint arXiv:2408.02138*, 2024.
- [29] L.-A. Zeng and W.-S. Zheng, "Multimodal action quality assessment," *IEEE TIP*, 2024.
- [30] S.-J. Zhang, J.-H. Pan, J. Gao, and W.-S. Zheng, "Semi-supervised action quality assessment with self-supervised segment feature recovery," *IEEE TCSVT*, vol. 32, no. 9, pp. 6017–6028, 2022.
- [31] W. Yun, M. Qi, F. Peng, and H. Ma, "Semi-supervised teacher-reference-student architecture for action quality assessment," *arXiv preprint arXiv:2407.19675*, 2024.
- [32] K. Zhou, L. Wang, X. Zhang, H. P. Shum, F. W. Li, J. Li, and X. Liang, "Magr: Manifold-aligned graph regularization for continual action quality assessment," *arXiv preprint arXiv:2403.04398*, 2024.
- [33] Y.-M. Li, L.-A. Zeng, J.-K. Meng, and W.-S. Zheng, "Continual action assessment via task-consistent score-discriminative feature distribution modeling," *IEEE TCSVT*, 2024.
- [34] A. Dadashzadeh, S. Duan, A. Whone, and M. Mirmehdi, "Pecop: Parameter efficient continual pretraining for action quality assessment," in *WACV*, pp. 42–52, 2024.
- [35] Y.-M. Li, A.-L. Wang, K.-Y. Lin, T. Yu-Ming, L.-A. Zeng, J.-F. Hu, and W.-S. Zheng, "Techcoach: Towards technical keypoint-aware descriptive action coaching," *arXiv preprint arXiv:2411.17130*, 2024.
- [36] A. Xu, L.-A. Zeng, and W.-S. Zheng, "Likert scoring with grade decoupling for long-term action assessment," in *CVPR*, pp. 3232–3241, 2022.
- [37] P. Parmar and B. T. Morris, "What and how well you performed? a multitask learning approach to action quality assessment," in *CVPR*, pp. 304–313, 2019.
- [38] Y. Liu, X. Cheng, and T. Ikenaga, "A figure skating jumping dataset for replay-guided action quality assessment," in *ACM MM*, pp. 2437–2445, 2023.
- [39] T. Wang, Y. Wang, and M. Li, "Towards accurate and interpretable surgical skill assessment: A video-based method incorporating recognized surgical gestures and skill levels," in *MICCAI*, pp. 668–678, Springer, 2020.
- [40] H. Doughty, D. Damen, and W. Mayol-Cuevas, "Who's better? who's best? pairwise deep ranking for skill determination," in *CVPR*, pp. 6057–6066, 2018.
- [41] M. Fang, X. Du, Q. Liu, Y. Zhou, Q. Liang, and S. Liu, "Which is the better teacher action? a new ranking model and dataset," in *ICASSP*, pp. 7695–7699, IEEE, 2024.
- [42] A. Krizhevsky, I. Sutskever, and G. E. Hinton, "Imagenet classification with deep convolutional neural networks," *NeurIPS*, vol. 25, 2012.
- [43] K. He, X. Zhang, S. Ren, and J. Sun, "Deep residual learning for image recognition," in *CVPR*, pp. 770–778, 2016.
- [44] D. Tran, L. Bourdev, R. Fergus, L. Torresani, and M. Paluri, "Learning spatiotemporal features with 3d convolutional networks," in *ICCV*, pp. 4489–4497, 2015.
- [45] Z. Qiu, T. Yao, and T. Mei, "Learning spatio-temporal representation with pseudo-3d residual networks," in *ICCV*, pp. 5533–5541, 2017.
- [46] J. Carreira and A. Zisserman, "Quo vadis, action recognition? a new model and the kinetics dataset," in *CVPR*, pp. 6299–6308, 2017.
- [47] Z. Liu, J. Ning, Y. Cao, Y. Wei, Z. Zhang, S. Lin, and H. Hu, "Video swin transformer," in *CVPR*, pp. 3202–3211, 2022.
- [48] S. Wang, D. Yang, P. Zhai, C. Chen, and L. Zhang, "Tsa-net: Tube self-attention network for action quality assessment," in *ACM MM*, pp. 4902–4910, 2021.
- [49] T. Nagai, S. Takeda, M. Matsumura, S. Shimizu, and S. Yamamoto, "Action quality assessment with ignoring scene context," in *ICIP*, pp. 1189–1193, IEEE, 2021.
- [50] J.-H. Pan, J. Gao, and W.-S. Zheng, "Action assessment by joint relation graphs," in *ICCV*, pp. 6331–6340, 2019.
- [51] J.-H. Pan, J. Gao, and W.-S. Zheng, "Adaptive action assessment," *IEEE TPAMI*, vol. 44, no. 12, pp. 8779–8795, 2021.
- [52] K. Gedamu, Y. Ji, Y. Yang, J. Shao, and H. T. Shen, "Self-supervised subaction parsing network for semi-supervised action quality assessment," *IEEE TIP*, 2024.
- [53] K. Gedamu, Y. Ji, Y. Yang, J. Shao, and H. T. Shen, "Fine-grained spatio-temporal parsing network for action quality assessment," *IEEE TIP*, vol. 32, pp. 6386–6400, 2023.
- [54] Z. Li, L. Gu, W. Wang, R. Nakamura, and Y. Sato, "Surgical skill assessment via video semantic aggregation," in *MICCAI*, pp. 410–420, Springer, 2022.
- [55] L. Okamoto and P. Parmar, "Hierarchical neurosymbolic approach for comprehensive and explainable action quality assessment," in *CVPRW*, pp. 3204–3213, 2024.
- [56] X. Dong, X. Liu, W. Li, A. Adeyemi-Ejeye, and A. Gilbert, "Interpretable long-term action quality assessment," *arXiv preprint arXiv:2408.11687*, 2024.
- [57] J. Xu, Y. Rao, X. Yu, G. Chen, J. Zhou, and J. Lu, "Finediving: A fine-grained dataset for procedure-aware action quality assessment," in *CVPR*, pp. 2949–2958, 2022.
- [58] Y. Bai, D. Zhou, S. Zhang, J. Wang, E. Ding, Y. Guan, Y. Long, and J. Wang, "Action quality assessment with temporal parsing transformer," in *ECCV*, pp. 422–438, Springer, 2022.
- [59] J. Xu, S. Yin, G. Zhao, Z. Wang, and Y. Peng, "Fineparser: A fine-grained spatio-temporal action parser for human-centric action quality assessment," in *CVPR*, pp. 14628–14637, 2024.
- [60] H. Matsuyama, N. Kawaguchi, and B. Y. Lim, "Iris: Interpretable rubric-informed segmentation for action quality assessment," in *ICIUI*, pp. 368–378, 2023.
- [61] Y. Tang, Z. Ni, J. Zhou, D. Zhang, J. Lu, Y. Wu, and J. Zhou, "Uncertainty-aware score distribution learning for action quality assessment," in *CVPR*, pp. 9839–9848, 2020.
- [62] C. Zhou, Y. Huang, and H. Ling, "Uncertainty-driven action quality assessment," *arXiv preprint arXiv:2207.14513*, 2022.
- [63] B. Zhang, J. Chen, Y. Xu, H. Zhang, X. Yang, and X. Geng, "Auto-encoding score distribution regression for action quality

- assessment," *Neural Computing and Applications*, vol. 36, no. 2, pp. 929–942, 2024.
- [64] Y. Ji, L. Ye, H. Huang, L. Mao, Y. Zhou, and L. Gao, "Localization-assisted uncertainty score disentanglement network for action quality assessment," in *ACM MM*, pp. 8590–8597, 2023.
- [65] K. Zhou, J. Li, R. Cai, L. Wang, X. Zhang, and X. Liang, "Cofinal: Enhancing action quality assessment with coarse-to-fine instruction alignment," in *IJCAI*, 2024.
- [66] M. Li, H.-B. Zhang, Q. Lei, Z. Fan, J. Liu, and J.-X. Du, "Pairwise contrastive learning network for action quality assessment," in *ECCV*, pp. 457–473, Springer, 2022.
- [67] X. Ke, H. Xu, X. Lin, and W. Guo, "Two-path target-aware contrastive regression for action quality assessment," *Information Sciences*, vol. 664, p. 120347, 2024.
- [68] Q. An, M. Qi, and H. Ma, "Multi-stage contrastive regression for action quality assessment," in *ICASSP*, pp. 4110–4114, IEEE, 2024.
- [69] Z. Luo, Y. Xiao, F. Yang, J. T. Zhou, and Z. Fang, "Rhythmer: Ranking-based skill assessment with rhythm-aware transformer," *IEEE TCSVT*, 2024.
- [70] Z. Cao, T. Simon, S.-E. Wei, and Y. Sheikh, "Realtime multi-person 2d pose estimation using part affinity fields," in *CVPR*, pp. 7291–7299, 2017.
- [71] C. Lugaresi, J. Tang, H. Nash, C. McClanahan, E. Ubowaja, M. Hays, F. Zhang, C.-L. Chang, M. G. Yong, J. Lee, et al., "Mediapipe: A framework for building perception pipelines," *arXiv preprint arXiv:1906.08172*, 2019.
- [72] Y. Xu, J. Zhang, Q. Zhang, and D. Tao, "Vitpose: Simple vision transformer baselines for human pose estimation," *NeurIPS*, vol. 35, pp. 38571–38584, 2022.
- [73] X. Wang, J. Li, and H. Hu, "Skeleton-based action quality assessment via partially connected lstm with triplet losses," in *PRCV*, pp. 220–232, Springer, 2022.
- [74] B. X. B. Yu, Y. Liu, X. Zhang, G. Chen, and K. C. C. Chan, "EGCN: an ensemble-based learning framework for exploring effective skeleton-based rehabilitation exercise assessment," in *IJCAI*, pp. 3681–3687, 2022.
- [75] X. Bruce, Y. Liu, K. C. Chan, and C. W. Chen, "Egcn++: A new fusion strategy for ensemble learning in skeleton-based rehabilitation exercise assessment," *IEEE TPAMI*, 2024.
- [76] C. Li, X. Ling, and S. Xia, "A graph convolutional siamese network for the assessment and recognition of physical rehabilitation exercises," in *ICANN*, pp. 229–240, Springer, 2023.
- [77] X. Bruce, Y. Liu, K. C. Chan, Q. Yang, and X. Wang, "Skeleton-based human action evaluation using graph convolutional network for monitoring alzheimer's progression," *PR*, vol. 119, p. 108095, 2021.
- [78] Y. Liao, A. Vakanski, and M. Xian, "A deep learning framework for assessing physical rehabilitation exercises," *IEEE TNSRE*, vol. 28, no. 2, pp. 468–477, 2020.
- [79] S. Yan, Y. Xiong, and D. Lin, "Spatial temporal graph convolutional networks for skeleton-based action recognition," in *AAAI*, vol. 32, 2018.
- [80] C. Zhou, J. Zeng, L. Qiu, S. Wang, P. Liu, and J. Pan, "An attention-based adaptive spatial-temporal graph convolutional network for long-video ergonomic risk assessment," *Engineering Applications of Artificial Intelligence*, vol. 131, p. 107780, 2024.
- [81] J. Xia, M. Zhuge, T. Geng, S. Fan, Y. Wei, Z. He, and F. Zheng, "Skating-mixer: Long-term sport audio-visual modeling with mlps," in *AAAI*, pp. 2901–2909, 2023.
- [82] Y. Zhong, F. Zhang, and Y. Demiris, "Contrastive self-supervised learning for automated multi-modal dance performance assessment," in *ICASSP*, pp. 1–5, IEEE, 2023.
- [83] S. Kondo, "Zeal: Surgical skill assessment with zero-shot tool inference using unified foundation model," *arXiv preprint arXiv:2407.02738*, 2024.
- [84] Z. Du, D. He, X. Wang, and Q. Wang, "Learning semantics-guided representations for scoring figure skating," *IEEE TMM*, 2023.
- [85] K. Gedamu, Y. Ji, Y. Yang, J. Shao, and H. T. Shen, "Visual-semantic alignment temporal parsing for action quality assessment," *IEEE TCSVT*, 2024.
- [86] S. Zahan, G. M. Hassan, and A. Mian, "Learning sparse temporal video mapping for action quality assessment in floor gymnastics," *IEEE Transactions on Instrumentation and Measurement*, 2024.
- [87] Y. Ding, S. Zhang, S. Liu, J. Zhang, W. Chen, D. Haifei, T. Sun, et al., "2m-af: A strong multi-modality framework for human action quality assessment with self-supervised representation learning," in *ACM MM*, 2024.
- [88] L. Dong, W. Wang, Y. Qiao, and X. Sun, "Lucidaction: A hierarchical and multi-model dataset for comprehensive action quality assessment," *NeurIPS*, 2025.
- [89] M. A. A. H. Khan and H. Shahriar, "Mrehab: Multimodal data acquisition and modeling framework for assessing stroke and cardiac rehabilitation exercises," in *COMPSAC*, pp. 452–453, IEEE, 2022.
- [90] D.-W. Kim, J. E. Park, M.-J. Kim, S. H. Byun, C. I. Jung, H. M. Jeong, S. R. Woo, K. H. Lee, M. H. Lee, J.-W. Jung, et al., "Automatic assessment of upper extremity function and mobile application for self-administered stroke rehabilitation," *TNSRE*, 2024.
- [91] Y. Huang, G. Chen, J. Xu, M. Zhang, L. Yang, B. Pei, H. Zhang, L. Dong, Y. Wang, L. Wang, et al., "Egoexolearn: A dataset for bridging asynchronous ego-and exo-centric view of procedural activities in real world," in *CVPR*, pp. 22072–22086, 2024.
- [92] P. Parmar and B. Morris, "Action quality assessment across multiple actions," in *WACV*, pp. 1468–1476, IEEE, 2019.
- [93] Y. Gao, S. S. Vedula, C. E. Reiley, N. Ahmidi, B. Varadarajan, H. C. Lin, L. Tao, L. Zappella, B. Béjar, D. D. Yuh, et al., "Jhu-isi gesture and skill assessment working set (jigsaws): A surgical activity dataset for human motion modeling," in *MICCAIW*, p. 3, 2014.
- [94] L.-A. Zeng, F.-T. Hong, W.-S. Zheng, Q.-Z. Yu, W. Zeng, Y.-W. Wang, and J.-H. Lai, "Hybrid dynamic-static context-aware attention network for action assessment in long videos," in *ACM MM*, pp. 2526–2534, 2020.
- [95] S. Zhang, W. Dai, S. Wang, X. Shen, J. Lu, J. Zhou, and Y. Tang, "Logo: A long-form video dataset for group action quality assessment," in *CVPR*, pp. 2405–2414, 2023.
- [96] S.-J. Zhang, J.-H. Pan, J. Gao, and W.-S. Zheng, "Adaptive stage-aware assessment skill transfer for skill determination," *TMM*, 2023.
- [97] K. Ashutosh, T. Nagarajan, G. Pavlakos, K. Kitani, and K. Grauman, "Expertaf: Expert actionable feedback from video," *arXiv preprint arXiv:2408.00672*, 2024.
- [98] P. Parmar and B. Tran Morris, "Learning to score olympic events," in *CVPRW*, pp. 20–28, 2017.
- [99] X. Ding, X. Xu, and X. Li, "Sedskill: Surgical events driven method for skill assessment from thoracoscopic surgical videos," in *MICCAI*, pp. 35–45, Springer Nature Switzerland Cham, 2023.
- [100] Y. Li, X. Chai, and X. Chen, "Scoringnet: Learning key fragment for action quality assessment with ranking loss in skilled sports," in *ACCV*, pp. 149–164, Springer, 2018.
- [101] Z. Li, Y. Huang, M. Cai, and Y. Sato, "Manipulation-skill assessment from videos with spatial attention network," in *ICCVW*, pp. 0–0, 2019.
- [102] D. Anastasiou, Y. Jin, D. Stoyanov, and E. Mazomenos, "Keep your eye on the best: contrastive regression transformer for skill assessment in robotic surgery," *IEEE Robotics and Automation Letters*, vol. 8, no. 3, pp. 1755–1762, 2023.
- [103] X. Xiang, Y. Tian, A. Reiter, G. D. Hager, and T. D. Tran, "S3d: Stacking segmental p3d for action quality assessment," in *ICIP*, pp. 928–932, IEEE, 2018.
- [104] H.-B. Zhang, L.-J. Dong, Q. Lei, L.-J. Yang, and J.-X. Du, "Label-reconstruction-based pseudo-subscore learning for action quality assessment in sporting events," *Applied Intelligence*, vol. 53, no. 9, pp. 10053–10067, 2023.
- [105] L.-J. Dong, H.-B. Zhang, Q. Shi, Q. Lei, J.-X. Du, and S. Gao, "Learning and fusing multiple hidden substages for action quality assessment," *Knowledge-Based Systems*, vol. 229, p. 107388, 2021.
- [106] C.-I. Joung, S. Byun, and S. Baek, "Contrastive learning for action assessment using graph convolutional networks with augmented virtual joints," *IEEE Access*, 2023.
- [107] J. Carreira, E. Noland, A. Banki-Horvath, C. Hillier, and A. Zisserman, "A short note about kinetics-600," *arXiv preprint arXiv:1808.01340*, 2018.
- [108] J. Xu, Y. Rao, J. Zhou, and J. Lu, "Procedure-aware action quality assessment: Datasets and performance evaluation," *IJCV*, pp. 1–22, 2024.
- [109] J. Gao, W.-S. Zheng, J.-H. Pan, C. Gao, Y. Wang, W. Zeng, and J. Lai, "An asymmetric modeling for action assessment," in *ECCV*, pp. 222–238, Springer, 2020.

- [110] J. Gao, J.-H. Pan, S.-J. Zhang, and W.-S. Zheng, "Automatic modelling for interactive action assessment," *IJCV*, vol. 131, no. 3, pp. 659–679, 2023.
- [111] W. Ilg, J. Mezger, and M. Giese, "Estimation of skill levels in sports based on hierarchical spatio-temporal correspondences," in *PR*, pp. 523–531, Springer, 2003.
- [112] K. Wnuk and S. Soatto, "Analyzing diving: A dataset for judging action quality," in *ACCV*, pp. 266–276, Springer, 2010.
- [113] H. Pirsiavash, C. Vondrick, and A. Torralba, "Assessing the quality of actions," in *ECCV*, pp. 556–571, Springer, 2014.
- [114] V. Venkataraman, I. Vlachos, and P. K. Turaga, "Dynamical regularity for action analysis," in *BMVC*, vol. 67, pp. 1–12, 2015.
- [115] Y. Sharma, V. Bettadapura, N. Hammerla, S. Mellor, R. McNaney, P. Olivier, S. Deshmukh, A. McCaskie, I. Essa, *et al.*, "Video based assessment of osats using sequential motion textures," in *Workshop on Modeling and Monitoring of Computer Assisted Interventions 2014*, Springer, 2014.
- [116] A. Zia, Y. Sharma, V. Bettadapura, E. L. Sarin, T. Ploetz, M. A. Clements, and I. Essa, "Automated video-based assessment of surgical skills for training and evaluation in medical schools," *International Journal of Computer Assisted Radiology and Surgery*, vol. 11, pp. 1623–1636, 2016.
- [117] M. J. Fard, S. Ameri, R. Darin Ellis, R. B. Chinnam, A. K. Pandya, and M. D. Klein, "Automated robot-assisted surgical skill evaluation: Predictive analytics approach," *International Journal of Medical Robotics and Computer Assisted Surgery*, vol. 14, no. 1, p. e1850, 2018.
- [118] L. Tao, A. Paiement, D. Damen, M. Mirmehdi, S. Hannuna, M. Camplani, T. Burghardt, and I. Craddock, "A comparative study of pose representation and dynamics modelling for online motion quality assessment," *Computer Vision and Image Understanding*, vol. 148, pp. 136–152, 2016.
- [119] P. Dollár, V. Rabaud, G. Cottrell, and S. Belongie, "Behavior recognition via sparse spatio-temporal features," in *IEEE International Workshop on Visual Surveillance and Performance Evaluation of Tracking and Surveillance*, pp. 65–72, IEEE, 2005.
- [120] I. Laptev, "On space-time interest points," *IJCV*, vol. 64, pp. 107–123, 2005.
- [121] I. Laptev, M. Marszalek, C. Schmid, and B. Rozenfeld, "Learning realistic human actions from movies," in *CVPR*, pp. 1–8, IEEE, 2008.
- [122] W. Kay, J. Carreira, K. Simonyan, B. Zhang, C. Hillier, S. Vijayanarasimhan, F. Viola, T. Green, T. Back, P. Natsev, *et al.*, "The kinetics human action video dataset," *arXiv preprint arXiv:1705.06950*, 2017.
- [123] K. Roditakis, A. Makris, and A. Argyros, "Towards improved and interpretable action quality assessment with self-supervised alignment," in *Proceedings of the 14th Pervasive Technologies Related to Assistive Environments Conference*, pp. 507–513, 2021.
- [124] J. Xu, G. Zhao, S. Yin, W. Zhou, and Y. Peng, "Finesports: A multi-person hierarchical sports video dataset for fine-grained action understanding," in *CVPR*, pp. 2173–2178, 2024.
- [125] Q. Wang, L. Zhang, L. Bertinetto, W. Hu, and P. H. Torr, "Fast online object tracking and segmentation: A unifying approach," in *CVPR*, pp. 1328–1338, 2019.
- [126] L. Chen, J. Zhang, W. Wu, C. Han, and H. Gao, "Long video scoring method fusing high-precision pose and spatio-temporal attention modules," in *APWeb-WAIM*, pp. 466–475, Springer, 2024.
- [127] H. Fang, W. Zhou, and H. Li, "End-to-end action quality assessment with action parsing transformer," in *VCIP*, pp. 1–5, IEEE, 2023.
- [128] W. Wang, H. Wang, Y. Hao, and Q. Wang, "Action quality assessment with multi-scale temporal attention mechanism," in *ICAACE*, pp. 247–251, IEEE, 2024.
- [129] L. Liu, P. Zhai, D. Zheng, and Y. Fang, "Multi-stage action quality assessment method," in *CRIS*, pp. 116–122, 2023.
- [130] Q. Lei, H. Zhang, and J. Du, "Temporal attention learning for action quality assessment in sports video," *Signal, Image and Video Processing*, vol. 15, no. 7, pp. 1575–1583, 2021.
- [131] K. He, G. Gkioxari, P. Dollár, and R. Girshick, "Mask r-cnn," in *ICCV*, pp. 2961–2969, 2017.
- [132] F. Huang and J. Li, "Assessing action quality with semantic-sequence performance regression and densely distributed sample weighting," *Applied Intelligence*, vol. 54, no. 4, pp. 3245–3259, 2024.
- [133] A. Vaswani, N. Shazeer, N. Parmar, J. Uszkoreit, L. Jones, A. N. Gomez, L. u. Kaiser, and I. Polosukhin, "Attention is all you need," in *NeurIPS* (I. Guyon, U. V. Luxburg, S. Bengio, H. Wallach, R. Fergus, S. Vishwanathan, and R. Garnett, eds.), vol. 30, Curran Associates, Inc., 2017.
- [134] W. Hongli and X. Yang, "Learning to score sign language with two-stage method," *arXiv preprint arXiv:2404.10383*, 2024.
- [135] Q. Lei, H. Li, H. Zhang, J. Du, and S. Gao, "Multi-skeleton structures graph convolutional network for action quality assessment in long videos," *Applied Intelligence*, vol. 53, no. 19, pp. 21692–21705, 2023.
- [136] P.-X. Lian and Z.-G. Shao, "Improving action quality assessment with across-staged temporal reasoning on imbalanced data," *Applied Intelligence*, vol. 53, no. 24, pp. 30443–30454, 2023.
- [137] W. Liu, D. Anguelov, D. Erhan, C. Szegedy, S. Reed, C.-Y. Fu, and A. C. Berg, "Ssd: Single shot multibox detector," in *ECCV*, pp. 21–37, Springer, 2016.
- [138] T. He, H. Liu, Z. Ni, Y. Li, X. Ma, C. Zhong, Y. Zhang, Y. Wang, and W. Lin, "Achieving procedure-aware instructional video correlation learning under weak supervision from a collaborative perspective," *IJCV*, pp. 1–26, 2024.
- [139] T. He, H. Liu, Y. Li, X. Ma, C. Zhong, Y. Zhang, and W. Lin, "Collaborative weakly supervised video correlation learning for procedure-aware instructional video analysis," in *AAAI*, vol. 38, pp. 2112–2120, 2024.
- [140] H. Doughty, W. Mayol-Cuevas, and D. Damen, "The pros and cons: Rank-aware temporal attention for skill determination in long videos," in *CVPR*, pp. 7862–7871, 2019.
- [141] G. Bertasius, H. Soo Park, S. X. Yu, and J. Shi, "Am i a baller? basketball performance assessment from first-person videos," in *ICCV*, pp. 2177–2185, 2017.
- [142] M. W. Boal, D. Anastasiou, F. Tesfai, W. Ghamrawi, E. Mazomenos, N. Curtis, J. W. Collins, A. Sridhar, J. Kelly, D. Stoyanov, *et al.*, "Evaluation of objective tools and artificial intelligence in robotic surgery technical skills assessment: a systematic review," *British Journal of Surgery*, vol. 111, no. 1, p. znad331, 2024.
- [143] Q. Li, Z. Cui, I. Kitahara, and R. Sagawa, "Precise gymnastic scoring from tv playback," in *GCCE*, pp. 412–415, IEEE, 2022.
- [144] M.-Z. Li, H.-B. Zhang, L.-J. Dong, Q. Lei, and J.-X. Du, "Gaussian guided frame sequence encoder network for action quality assessment," *Complex & Intelligent Systems*, vol. 9, no. 2, pp. 1963–1974, 2023.
- [145] K. Sohn, H. Lee, and X. Yan, "Learning structured output representation using deep conditional generative models," *NeurIPS*, vol. 28, 2015.
- [146] D. P. Kingma, "Auto-encoding variational bayes," *arXiv preprint arXiv:1312.6114*, 2013.
- [147] H. Jain, G. Harit, and A. Sharma, "Action quality assessment using siamese network-based deep metric learning," *IEEE TCSVT*, vol. 31, no. 6, pp. 2260–2273, 2020.
- [148] Q. Lei, H.-B. Zhang, J.-X. Du, T.-C. Hsiao, and C.-C. Chen, "Learning effective skeletal representations on rgb video for fine-grained human action quality assessment," *Electronics*, vol. 9, no. 4, p. 568, 2020.
- [149] Z. Li, H. Chen, J. Cai, and Y. Xue, "Segmentation and quality assessment of continuous fitness movements based on vision," in *International Conference on Intelligent Computing*, pp. 96–107, Springer, 2024.
- [150] U. Gallardo, F. Caro, E. Hernández, R. Espinosa, and G. Ochoa-Ruiz, "Gymetricpose: A light-weight angle-based graph adaptation for action quality assessment," in *CBMS*, pp. 43–50, IEEE, 2024.
- [151] H.-Y. Li, Q. Lei, H.-B. Zhang, and J.-X. Du, "Skeleton based action quality assessment of figure skating videos," in *ITME*, pp. 196–200, IEEE, 2021.
- [152] T. Wang, M. Jin, J. Wang, Y. Wang, and M. Li, "Towards a data-driven method for rgb video-based hand action quality assessment in real time," in *Annual ACM Symposium on Applied Computing*, pp. 2117–2120, 2020.
- [153] B. Garg, A. Postlmayr, P. Cosman, and S. Dey, "Short: Deep learning approach to skeletal performance evaluation of physical therapy exercises," in *ACM/IEEE CHASE*, pp. 168–172, 2023.
- [154] A. Kryeem, S. Raz, D. Eluz, D. Itah, H. Hel-Or, and I. Shimshoni, "Personalized monitoring in home healthcare: An assistive system for post hip replacement rehabilitation," in *ICCV*, pp. 1868–1877, 2023.
- [155] A. Abedi, M. Malmirian, and S. S. Khan, "Cross-modal video to body-joints augmentation for rehabilitation exercise quality assessment," *arXiv preprint arXiv:2306.09546*, 2023.

- [156] F. Sardari, A. Paiement, S. Hannuna, and M. Mirmehdi, "View-invariant quality of human movement assessment," *Sensors*, vol. 20, no. 18, p. 5258, 2020.
- [157] C. Du, S. Graham, C. Depp, and T. Nguyen, "Assessing physical rehabilitation exercises using graph convolutional network with self-supervised regularization," in *EMBC*, pp. 281–285, IEEE, 2021.
- [158] S.-E. Wei, V. Ramakrishna, T. Kanade, and Y. Sheikh, "Convolutional pose machines," in *CVPR*, pp. 4724–4732, 2016.
- [159] M. Contributors, "Openmmlab pose estimation toolbox and benchmark." <https://github.com/open-mmlab/mmpose>, 2020.
- [160] K. Isakov, E. Burkov, V. Lempitsky, and Y. Malkov, "Learnable triangulation of human pose," in *ICCV*, pp. 7718–7727, 2019.
- [161] K. Zheng, J. Wu, J. Zhang, and C. Guo, "A skeleton-based rehabilitation exercise assessment system with rotation invariance," *IEEE TNSRE*, vol. 31, pp. 2612–2621, 2023.
- [162] S. Mehraban, V. Adeli, and B. Taati, "Motionagformer: Enhancing 3d human pose estimation with a transformer-gcnformer network," in *WACV*, pp. 6920–6930, 2024.
- [163] C. Zimmermann and T. Brox, "Learning to estimate 3d hand pose from single rgb images," in *ICCV*, pp. 4903–4911, 2017.
- [164] D. Pavlo, C. Feichtenhofer, D. Grangier, and M. Auli, "3d human pose estimation in video with temporal convolutions and semi-supervised training," in *ICCV*, pp. 7753–7762, 2019.
- [165] A. Zafir, E. Marinou, M. Zanfir, A.-I. Popa, and C. Sminchisescu, "Deep network for the integrated 3d sensing of multiple people in natural images," *NeurIPS*, vol. 31, 2018.
- [166] S. Deb, M. F. Islam, S. Rahman, and S. Rahman, "Graph convolutional networks for assessment of physical rehabilitation exercises," *IEEE TNSRE*, vol. 30, pp. 410–419, 2022.
- [167] L. Yao, Q. Lei, H. Zhang, J. Du, and S. Gao, "A contrastive learning network for performance metric and assessment of physical rehabilitation exercises," *IEEE TNSRE*, 2023.
- [168] J. Li, J. Xue, R. Cao, X. Du, S. Mo, K. Ran, and Z. Zhang, "Finerehab: A multi-modality and multi-task dataset for rehabilitation analysis," in *CVPRW*, pp. 3184–3193, 2024.
- [169] A. Kanade, M. Sharma, and M. Muniyandi, "Attention-guided deep learning framework for movement quality assessment," in *ICASSP*, pp. 1–5, IEEE, 2023.
- [170] M. Nekoui and L. Cheng, "Enhancing human motion assessment by self-supervised representation learning," in *BMVC*, p. 322, 2021.
- [171] T. Nagai, S. Takeda, S. Suzuki, and H. Seshimo, "Mmw-aqa: Multimodal in-the-wild dataset for action quality assessment," *IEEE Access*, 2024.
- [172] S. Hirose, T. Kato, T. Yamashita, and Y. Aoki, "Action quality assessment model using specialists' gaze location and kinematics data—focusing on evaluating figure skating jumps," *Sensors*, vol. 23, no. 22, p. 9282, 2023.
- [173] Z. Chen, W. Sun, Y. Tian, J. Jia, Z. Zhang, J. Wang, R. Huang, X. Min, G. Zhai, and W. Zhang, "Gaia: Rethinking action quality assessment for ai-generated videos," *arXiv preprint arXiv:2406.06087*, 2024.
- [174] A. Vakanski, H.-p. Jun, D. Paul, and R. Baker, "A data set of human body movements for physical rehabilitation exercises," *Data*, vol. 3, no. 1, p. 2, 2018.
- [175] J. Li, H. Hu, Q. Xing, X. Wang, J. Li, and Y. Shen, "Tai chi action quality assessment and visual analysis with a consumer rgb-d camera," in *MMSP*, pp. 1–6, IEEE, 2022.
- [176] L. Wang, J. Xie, X. Zhang, M. Huang, H. Su, and J. Zhu, "Hierarchical decomposition of prompt-based continual learning: Rethinking obscured sub-optimality," *NeurIPS*, vol. 36, 2024.
- [177] Q. Wang, L. Zhan, P. Thompson, and J. Zhou, "Multimodal learning with incomplete modalities by knowledge distillation," in *ACM SIGKDD*, pp. 1828–1838, 2020.
- [178] R. Guo, L. Cheng, J. Li, P. R. Hahn, and H. Liu, "A survey of learning causality with data: Problems and methods," *ACM Computing Surveys*, vol. 53, no. 4, pp. 1–37, 2020.
- [179] Z. Zhang, W. Sun, X. Li, Y. Li, Q. Ge, J. Jia, Z. Zhang, Z. Ji, F. Sun, S. Jui, *et al.*, "Human-activity agv quality assessment: A benchmark dataset and an objective evaluation metric," *arXiv preprint arXiv:2411.16619*, 2024.
- [180] Y.-M. Li, W.-J. Huang, A.-L. Wang, L.-A. Zeng, J.-K. Meng, and W.-S. Zheng, "Egoexo-fitness: Towards egocentric and exocentric full-body action understanding," *arXiv preprint arXiv:2406.08877*, 2024.

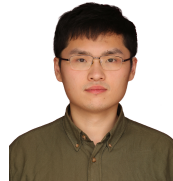
- [181] Z. Lu, H. Wang, Z. Chang, G. Yang, and H. P. Shum, "Hard no-box adversarial attack on skeleton-based human action recognition with skeleton-motion-informed gradient," in *ICCV*, pp. 4597–4606, 2023.



Kanglei Zhou is a Ph.D. candidate in the School of Computer Science and Engineering at Beihang University, specializing in action quality assessment and augmented reality. From February to August 2024, he was a visiting student in the Department of Computer Science at Durham University. He received his Bachelor's degree in the College of Computer and Information Engineering from Henan Normal University in 2020.



Ruizhi Cai received a B.Eng. degree in computer science and engineering at the School of Computer Science and Engineering at Beihang University. Now, he is pursuing a master's degree in software engineering at the same school of Beihang University. He is currently engaged in human motion analysis and action quality assessment.



Liyuan Wang received the B.S. and Ph.D. degrees from Tsinghua University. He is currently a postdoc at the Department of Computer Science and Technology, Tsinghua University. His research interests include continual learning, incremental learning, lifelong learning, and brain-inspired AI. His work has been published in major conferences and journals in related fields, such as Nature Machine Intelligence, TPAMI, NeurIPS, ICLR, CVPR, ICCV, ECCV, etc.



Hubert P. H. Shum (Senior Member, IEEE) is a Professor of Visual Computing and the Director of Research of the Department of Computer Science at Durham University, specialising in modelling spatio-temporal information with responsible AI. He is also a Co-Founder and the Co-Director of Durham University Space Research Centre. Before this, he was an Associate Professor/Senior Lecturer at Northumbria University and a Postdoctoral Researcher at RIKEN Japan. He received his PhD degree from the University of Edinburgh. He chaired conferences such as Pacific Graphics, BMVC and SCA, and has authored over 180 research publications.



Xiaohui Liang received his Ph.D. degree in computer science and engineering from Beihang University, China. He is currently a Professor, working in the School of Computer Science and Engineering at Beihang University. His main research interests include computer graphics and animation, visualization, and virtual reality.